International Journal of Control

ISSN: (Print) (Online) Journal homepage: www.tandfonline.com/journals/tcon20

Actuator fault detection and isolation in a class of nonlinear interconnected systems

Hamed Tirandaz, Christodoulos Keliris & Marios Polycarpou

To cite this article: Hamed Tirandaz, Christodoulos Keliris & Marios Polycarpou (2024) Actuator fault detection and isolation in a class of nonlinear interconnected systems, International Journal of Control, 97:12, 2914-2934, DOI: 10.1080/00207179.2024.2310606

To link to this article: https://doi.org/10.1080/00207179.2024.2310606

Published online: 06 Feb 2024.

Submit your article to this journal

Article views: 211

View related articles

View Crossmark data

Full Terms & Conditions of access and use can be found at
https://www.tandfonline.com/action/journalInformation?journalCode=tcon20

INTERNATIONAL JOURNAL OF CONTROL
2024, VOL. 97, NO. 12, 2914–2934
https://doi.org/10.1080/00207179.2024.2310606

Taylor & Francis
Taylor & Francis Group

Check for updates

Actuator fault detection and isolation in a class of nonlinear interconnected systems

Hamed Tirandaz, Christodoulos Keliris and Marios Polycarpou

KIOS Research Center for Intelligent Systems and Networks, Department of Electrical and Computer Engineering, University of Cyprus, Nicosia, Cyprus

ABSTRACT

In this paper, the problem of actuator fault detection and isolation is investigated for a class of nonlinear interconnected large-scale systems with modelling uncertainty and measurement noise, where each subsystem can have multiple inputs and multiple outputs (MIMO). The main contribution of this work is the derivation of a scheme that is able to diagnose single or multiple actuator faults in one or multiple subsystems. Each subsystem is monitored by a local diagnosis agent which contains the actuator fault detection module and the isolation module. The detection threshold in the fault detection module is generated through the use of a novel filtering technique, while the fault isolation module is realised by applying a reasoning-based decision logic based on a fault signature matrix. Fault propagation among subsystems is investigated and the results obtained allow for the identification of the subsystems that contain the faulty actuators. Finally, the effectiveness of the proposed actuator fault diagnosis method is demonstrated through a simulation example.

ARTICLE HISTORY
Received 13 September 2022
Accepted 30 December 2023

KEYWORDS
Nonlinear systems; actuator faults; fault detection and isolation (FDI); fault propagation

1. Introduction

1.1 Motivation

Abnormal operation or malfunction of actuators can cause unpredictable behaviour or even catastrophic consequences in dynamical systems, especially in large-scale infrastructure systems such as power generation and distribution systems, telecommunication networks, and water distribution networks. Thus, there is a need to develop efficient an effective fault detection and isolation (FDI) methods for such large-scale systems, especially for interconnected systems with multiple inputs and outputs. Hence, this work addresses the issue of actuator fault detection and isolation in large-scale interconnected nonlinear systems. Specifically, in this paper, actuator fault diagnosis is investigated via the analytical redundancy relation (ARR) approach and a distributed scheme is developed to detect and isolate multiple actuator faults in such systems.

Generally, fault detection and isolation in the analytical redundancy-related approaches can be categorised into centralised, decentralised, and distributed frameworks. In this regard, the reader can refer to J. Chen and Patton (2012), Reppa et al. (2016), Isermann (2006), Blanke et al. (2006), Ding (2008) and the reference therein, which mainly rely on model-based FDI approaches. Most research works on the FDI problem focus on a centralised framework. For instance, some centralised frameworks developed to address the FDI problem in linear dynamical systems are: a bank of unknown input observers utilised for FDI in linear systems is presented in Phatak and Viswanadham (1988); a lifting-based approach is designed in P. Zhang et al. (2012) for fault detection in linear periodic systems; model-based FDI in linear dynamical systems in a unified framework is given in J. Chen and Patton (2012); a set-theoretic unknown input observer scheme for robust FDI in linear systems is developed in Xu et al. (2017); a geometric approach for FDI in linear structured systems is presented in Jia et al. (2020); and a set-based geometric approach for FDI in uncertain linear systems is introduced in Z. Zhang and He (2022). Furthermore, there are many works in the literature that are devoted to the FDI problem in nonlinear dynamical systems, such as: sensor fault isolation in a class of MIMO nonlinear systems is proposed in Du and Mhaskar (2014) and its extension to deal with the actuator and sensor fault isolation problem is given in Du et al. (2013); a sliding mode scheme is developed for actuator FDI in a class of nonlinear systems in Yan and Edwards (2008a); actuator fault diagnosis for a class of active suspension systems is given in Mao et al. (2016); learning approaches which apply adaptive approximation models are presented in Polycarpou and Helmicki (1995) and Trunov and Polycarpou (2000); and nonlinear estimation techniques are investigated in Caccavale et al. (2008), Talebi et al. (2009), and Thumati and Jagannathan (2010).

Despite impressive development and widespread adoption of centralised FDI schemes, these schemes still face significant challenges, especially in large-scale interconnected systems. These include the vulnerability to security threats, short-communication-range capabilities, fault propagation issues, and challenges related to the computational complexity of large-scale interconnected systems. Non-centralised schemes are more suitable for dealing with these challenges since they take into consideration the interconnections between subsystems (Reppa et al., 2016). For example, the problem of FDI via a non-centralised framework for the case of linear systems

CONTACT Marios Polycarpou mpolycar@ucy.ac.cy KIOS Research Center for Intelligent Systems and Networks, Department of Electrical and Computer Engineering, University of Cyprus, Nicosia 1678, Cyprus

© 2024 Informa UK Limited, trading as Taylor & Francis Group

is widely investigated; see for example, Wang et al. (1997), Meskin and Khorasani (2009), Davoodi et al. (2013) and Li et al. (2017); however, there is limited research on large-scale nonlinear interconnected systems, i.e. Yin and Liu (2017), X. Zhang and Zhang (2012), Keliris et al. (2017) and Kougiatsos et al. (2022).

1.2 State-of-the-art

This work focuses on a distributed FDI approach for actuator faults in large-scale nonlinear interconnected systems. Among the non-centralised FDI schemes for large-scale interconnected nonlinear systems, there are very few results which are devoted to the problem of actuator FDI in such systems. For example, a sliding mode observer-based scheme is introduced in Yan and Edwards (2008b) for decentralised actuator fault detection and estimation in a class of large-scale systems. A distributed scheme for the FDI approach, based on neural networks, is proposed in X. Zhang and Zhang (2012) for process and actuator FDI in a class of interconnected uncertain nonlinear systems. An adaptive threshold technique which is designed to enhance the robustness against model uncertainties and noise at the decision-making stage for distributed FDI in a class of interconnected nonlinear systems, is designed in Keliris et al. (2013). In Boem, Ferrari, Keliris, et al. (2016), a distributed FDI scheme for nonlinear uncertain large-scale discrete-time systems is proposed for process and actuator faults, by using a filtering approach to reduce the effect of measurement noise. In Papadopoulos et al. (2017), the authors used an HVAC (heating, ventilation, and air conditioning) system as a network of interconnected subsystems and developed a distributed fault diagnosis scheme to detect actuator and sensor faults. A distributed scheme for actuator and sensor fault detection is proposed in Yin and Liu (2017), by considering a class of large-scale systems without any modelling uncertainty in the system structure. It must be noted that various works and developed methods for the FDI problem are performed under specific assumptions regarding the modelling uncertainty, noise, and system dynamic properties. As a result, a comparison amongst the various developed diagnosis methods is hard to be made. Some typical works are provided in Jung et al. (2015) and Bartys (2015a) which compare methods under the same conditions, i.e. without noise and modelling uncertainty.

In addition, many of the developed methods for actuator fault diagnosis consider a special form of systems, such that the actuators have distinct effects on the system functions. These methods however, may not be able to deal with systems with modelling uncertainties in either the local system functions or the system interconnection functions. For instance, many works consider affine systems, where actuator faults cannot affect the systems' functions, due to the fact that the system functions do not include the inputs. Furthermore, the majority of these works consider only a single actuator fault. However, there are a few research works in the literature devoted to the problem of multiple actuator fault diagnosis in large-scale interconnected nonlinear systems, such as Koscielny et al. (2011) and Koscielny and Bartys (2009), which consider only actuator fault isolation in their diagnosis schemes. The challenge is that the diagnosis of multiple faults turns out to be more complex than considering just a single fault. But in practice, in many diagnostic systems it is usually impossible to immediately detect and isolate faults. And also, as time progresses, observing single faults at distinct times in a system should be considered as multiple faults occurrence, something that is usually overseen in many works, since they only deal with a single fault.

As mentioned earlier, and inspired by the work of Keliris et al. (2015a), the residual generation and the fault detection scheme in this paper are designed such that an actuator fault in a subsystem can only be detected by the corresponding agent that monitors the subsystem for faults and not by any other agent of a neighbouring subsystem. As a result, when an actuator fault is detected by the fault detection module of the corresponding FDI agent it is guaranteed that the fault has occurred in the subsystem the agent monitors. Then, the fault isolation module of that FDI agent is activated to isolate the detected fault among the actuators of that subsystem.

Generally, the most common approach for fault isolation in analytical redundancy relation-based methods, is by using a signature matrix to assign the different sets of actuators/sensors some likely fault patterns. The fault signature matrix represents the sensitivity of the ARRs to every fault combination. References Koscielny et al. (2011), Kościelny (1995), De Kleer and Kurien (2003), Reppa et al. (2014a) and Bartys (2015b) have investigated the fault isolation problem based on a structure of the signature matrix, but the actuator fault isolation problem still carries challenges. In fact, as it is stated in J. Chen and Patton (2012), actuator fault isolation is not always possible. Moreover, the task of isolating multiple actuator faults, especially in the case of large-scale interconnected nonlinear dynamical systems, has not been significantly investigated by the research community.

1.3 Key contributions

Motivated by the above discussion, the focus of this paper is to study the problem of multiple actuator fault diagnosis in a class of interconnected nonlinear systems, with multiple inputs per subsystem, subject to possibly multiple actuator faults in a single or multiple subsystems, via a distributed FDI framework. Each subsystem is monitored by its corresponding FDI agent, which contains two modules: the actuator fault detection module, which generates an adaptive fault detection threshold, and the actuator fault isolation module, which is initiated after the detection of a fault in the local module and is responsible for isolating the potential faulty actuators. The FDI agents communicate between them by mirroring the system interconnections. The main contribution of this paper is the derivation of an actuator fault diagnosis scheme dealing with multiple actuator faults in a distributed way which encompasses the following three important characteristics:

(a) The fault detection threshold generation is constructed using a novel filtering technique.
(b) Immediate identification of the subsystem(s) containing the faulty actuator(s), once a fault is detected. Generally, the fault propagation problem constitutes an important challenge in fault diagnosis in decentralised or distributed systems. For instance, in the case of actuator fault propagation,

an actuator fault in one subsystem may affect the neighbouring subsystems through the interconnection variables that are contaminated by the fault effects. One work that deals with the fault propagation problem and has investigated the process and the sensor fault propagation in distributed interconnected systems is Keliris et al. (2015a). This paper deals with the actuator fault propagation problem and exploits the findings to allow for multiple actuator fault diagnosis. Specifically, when the detection module of an FDI agent detects a fault in the respective subsystem that is being monitored, then it is guaranteed that the actuator fault(s) is/are contained in the corresponding subsystem, and not in a neighbouring subsystem.

(c) A reasoning-based decision logic scheme is designed to isolate single/multiple faults within each faulty subsystem. In this work, instead of a binary signature matrix indicating the presence or not of a fault in the system state variables, a four-valued signature matrix, based on the effects of the actuators faults on the behaviour of the system state variables is developed and is used for isolation purposes. Finally, a new type of evaluation of the signature matrix, named as Set-Enumeration tree (SE-tree) evaluation, which was originally developed in Rymon (1993), is performed in order to reduce the computational complexity in systems with a large signature matrix. As a result, the proposed scheme is able to isolate the faulty actuators, of each identified faulty subsystem, either uniquely or in at least a subset of the subsystem actuators.

1.4 Overview

The organisation of this paper is as follows: Section 2 presents the problem formulation, and Section 3 contains the analysis of the actuator fault detection strategy and the actuator fault detectability analysis. The problem of fault propagation is studied in Section 4 and actuator fault isolation is investigated in Section 5. Simulation results are presented in Section 6. Finally, some concluding remarks are given in Section 7.

Notation: The notation $|\cdot|$ denotes the absolute value of a scalar and $\|\cdot\|$ stands for the Euclidean norm of a vector.

2. Problem formulation

In this paper, we consider a class of nonlinear systems composed of N interconnected subsystems, $I \in \{1, \ldots, N\}$. The dynamics of the Ith subsystem $\Sigma^{(I)}$ are given by:

$$\Sigma^{(I)}: \begin{cases} \dot{x}^{(I)}(t) = A^{(I)}x^{(I)}(t) + g^{(I)}\left(x^{(I)}(t), u^{(I)}(t)\right) \\ \quad +h^{(I)}\left(x^{(I)}(t), z^{(I)}(t), u^{(I)}(t)\right) \\ \quad +\eta^{(I)}\left(x^{(I)}(t), z^{(I)}(t), t\right) \\ y^{(I)}(t) = x^{(I)}(t) + \xi_y^{(I)}(t), \end{cases} \tag{1}$$

where $x^{(I)} \in \mathbb{R}^{n_I}$, $u^{(I)} \in \mathbb{R}^{m_I}$ and $y^{(I)} \in \mathbb{R}^{n_I}$ denote the state, input and the output vectors of the Ith subsystem, respectively and $z^{(I)} \in \mathbb{R}^{\bar{n}_I}$ represents the set of interconnection variables, i.e. the states of the other subsystems that affect the Ith subsystem. The matrix $A^{(I)} \in \mathbb{R}^{n_I \times n_I}$ represents the known local linear part of the Ith subsystem and $g^{(I)}: \mathbb{R}^{n_I} \times \mathbb{R}^{m_I} \to \mathbb{R}^{n_I}$ the known local nonlinear part of the function dynamics of the Ith subsystem; $h^{(I)}: \mathbb{R}^{n_I} \times \mathbb{R}^{\bar{n}_I} \times \mathbb{R}^{m_I} \to \mathbb{R}^{n_I}$ represents the known part of the interconnection function of the Ith subsystem; $g^{(I)}$ and $h^{(I)}$ are considered as differentiable functions with respect to variables $x^{(I)}$, $x^{(I)}$ and $z^{(I)}$, respectively. As a result, $g_i^{(I)}$ (ith element of $g^{(I)}$) is Lipschitz with respect to variable $x^{(I)}$ and has Lipschitz constant $L_{g_i^{(I)}}$ which is considered known. Also, $h_i^{(I)}$ (ith element of $h^{(I)}$) is Lipschitz with known Lipschitz constants $L^{(x)}_{h_i^{(I)}}$ and $L^{(z)}_{h_i^{(I)}}$ with respect to variables $x^{(I)}$ and $z^{(I)}$, respectively, for all $i = 1, \ldots, n_I$. The vector $\xi_y^{(I)}(t) \triangleq [\xi_{y,1}^{(I)}(t), \ldots, \xi_{y,n_I}^{(I)}(t)]^T \in \mathbb{R}^{n_I}$ is the (bounded) measurement noise vector and, $\eta^{(I)}: \mathbb{R}^{n_I} \times \mathbb{R}^{\bar{n}_I} \times \mathbb{R}^{+} \to \mathbb{R}^{n_I}$ characterises the unknown modelling uncertainty, disturbances and also possibly uncertain interconnections of the Ith subsystem. It is noted that the uncertainty function $\eta^{(I)}$ is not only unknown but it may also be time-varying. Note that, the system representation given by (1), where local linear, nonlinear and interconnection function dynamics are considered known whereas all uncertainties are grouped in one unknown function term is considered in several other works, e.g. Talebi et al. (2009), Boem et al. (2013), Reppa et al. (2014a, 2014b), Papadopoulos et al. (2017), W. Chen et al. (2013), Khalili et al. (2019), L. Zhang et al. (2020), Kougiatsos et al. (2022), X. Zhang and Zhang (2012) and X. Zhang (2011).

Remark 2.1: In this work, we consider a class of nonlinear systems composed of N interconnected subsystems as indicated by Equation (1) which refers to full-state measurement along with some measurement noise. Considering full state measurement allows for more accurate fault isolation results in comparison to having partial state measurement and allows us to focus better on the core isolation problem rather than having to deal with the additional problem of not having available all states. In general, in fault diagnosis literature of nonlinear systems, it is common to consider full state measurement (along with possibly measurement noise), like in works by Arrichiello et al. (2015), X. Zhang et al. (2002), Ferrari et al. (2009), Boem, Ferrari, Parisini (2011), Boem, Ferrari, Keliris, et al. (2016), Papadopoulos et al. (2017), W. Chen et al. (2013), Ferdowsi et al. (2014), Khalili et al. (2019) and Kougiatsos et al. (2022).

Lemma 2.1: *There exists a known constant $L_{h_i^{(I)}}$ such that*

$$\begin{aligned} &\left|h_i^{(I)}(x^{(I)}, z^{(I)}, u^{(I)}) - h_i^{(I)}(\hat{x}^{(I)}, y_z^{(I)}, u^{(I)})\right| \\ &\quad \le L_{h_i^{(I)}}\left(\left\|x^{(I)} - \hat{x}^{(I)}\right\| + \bar{\xi}_z^{(I)}\right) \\ &\quad \forall\, x^{(I)}, \hat{x}^{(I)} \in \mathcal{X}, z^{(I)}, y_z^{(I)} \in Z, \quad i = 1, \ldots, n_I, \end{aligned}$$

where $\mathcal{X}$ and Z are the compact subsets of $\mathbb{R}^{n_I}$ and $\mathbb{R}^{\bar{n}_I}$, respectively and $\bar{\xi}_z^{(I)}$ is a bound on $\xi_z^{(I)} \triangleq y_z^{(I)} - z^{(I)}$, (where $y_z^{(I)}$ denotes the output vector associated with $z(t)$, i.e. $y_z^{(I)} = z^{(I)} + \xi_z^{(I)}$) i.e. $\|\xi_z^{(I)}\| \le \bar{\xi}_z^{(I)}$; and $L_{h_i^{(I)}} \triangleq \max\{L^{(x)}_{h_i^{(I)}}, L^{(z)}_{h_i^{(I)}}\}$.

Proof: Since $h_i^{(I)}$ is considered Lipschitz in variables $x^{(I)}$ and $z^{(I)}$, the proof is straightforward and is therefore omitted (it

is based on the Lipschitz conditions on each variable and the triangle inequality). ■

Remark 2.2: The level of interconnection function $h^{(I)}$ is related to the Lipschitz constant associated in Lemma 2.1. Furthermore, the effects of the interconnection term $h^{(I)}$ (and consequently of the level of the interconnection) on the adaptive fault detection threshold that will be designed in the sequel, will appear as the Lipschitz constant $L_{h^{(I)}}$ and the bound on the measurement noise of the interconnected variables $\bar{\xi}^{(I)}$. Hence, all the interconnection function effects are taken into consideration for the derivation of the detection threshold.

In many situations, faults can only affect a system in a certain way (i.e. leakages often induce a mass flow following a pressure gradient). Therefore, in this paper, we consider the actuator faults that cause some loss of effectiveness on the actuators performance in a system. Specifically, the actuator output $u_i^{(I)}$ (ith element of $u^{(I)}$) is modelled similarly to X. Zhang et al. (2002), as follows:

$$u_i^{(I)}(t) = \beta_i^{(I)}(t - T_{0,i}^{(I)})\, u_{H,i}^{(I)}(t), \quad i = 1, \ldots, m_I, \tag{2}$$

where $u_{H,i}^{(I)}$ is the ith element of $u_H^{(I)} : \mathbb{R}^+ \to \mathbb{R}^{m_I}$ and denotes the healthy control input of the ith actuator; $T_{0,i}^{(I)} \in \mathbb{R}^+$ indicates the unknown occurrence time of the fault in the ith actuator of the Ith subsystem and $\beta_i^{(I)}(t - T_{0,i}^{(I)})$ $i = 1, \ldots, m_I$ denotes the unknown time profile of the ith actuator fault, indicating the loss of actuator effectiveness. Specifically, in this paper, we consider exponentially decaying faults with a bias (to account for constant loss of performance), modelled as

$$\beta_i^{(I)}(t - T_{0,i}^{(I)}) = \begin{cases} 1 & \forall\, t \le T_{0,i}^{(I)} \\ \alpha_i^{(I)} + (1 - \alpha_i^{(I)})\, \mathrm{e}^{-\lambda_i^{(I)}\left(t - T_{0,i}^{(I)}\right)} & \forall\, t > T_{0,i}^{(I)}, \end{cases} \tag{3}$$

where $\alpha_i^{(I)} \in [0, 1]$, $i = 1, \ldots, m_I$ denotes the final percentage of loss of effectiveness of the ith actuator of the Ith subsystem and $\lambda_i^{(I)} \in (0, \infty]$ is the unknown fault evolution rate. As the magnitude of $\alpha_i^{(I)}$ decreases the actuator loss of effectiveness increases. If $\alpha_i^{(I)} = 0$, then the actuator at some time becomes out of order. Furthermore, the parameter $\lambda_i^{(I)}$ affects the time profile $\beta_i^{(I)}$ such that incipient faults result from small values of $\lambda_i^{(I)}$ whereas abrupt faults result from larger values of $\lambda_i^{(I)}$. In general, incipient faults are more difficult to detect than abrupt faults. Note that the function $\beta_i^{(I)}(t - T_{0,i}^{(I)})$ in (3) ranges from 1 (healthy) to 0 (out of order).

In the sequel, $T_0^{(I)}$ indicates the occurrence time of the first actuator fault in the Ith subsystem.

The following assumptions are used in this work.

Assumption 2.1 (well-posedness): *The state vector $x^{(I)}(t)$, $I = 1, \ldots, N$ remains bounded before and after the occurrence of any actuator fault, i.e. $x^{(I)}(t) \in L_\infty$ $\forall\, t \ge 0$.*

The above assumption is required for well-posedness since in this work we deal with the fault detection and isolation problem (not with the feedback control and fault accommodation problems). It is worth mentioning that, the proposed distributed FDI design is independent of the control and accommodation task. Note that, although the states are considered to be bounded, a bound is not considered or required to be known. This assumption is commonly found in other fault diagnosis works, such as Boem, Ferrari, Parisini (2011), Boem, Ferrari, Keliris, et al. (2016), Papadopoulos et al. (2017), Reppa et al. (2014a), Riverso et al. (2016), X. Zhang and Zhang (2012), X. Zhang (2011) and Keliris et al. (2015b).

Assumption 2.2: *Each element of the unknown modelling uncertainty function $\eta^{(I)}$ is (possibly) unconstructed and bounded by:*

$$\left|\eta_i^{(I)}(x^{(I)}, z^{(I)}, t)\right| \le \bar{\eta}_i^{(I)}(x^{(I)}, y_z^{(I)}), \quad \forall\, i = 1, \ldots, n_I, \tag{4}$$

where $\bar{\eta}_i^{(I)}$ is a known, positive, uniformly bounding function with respect to t and, locally Lipschitz with respect to $x^{(I)}$ as follows:

$$\begin{aligned} &\left|\bar{\eta}_i^{(I)}(x^{(I)}, y_z{}^{(I)}) - \bar{\eta}_i^{(I)}(\hat{x}^{(I)}, y_z{}^{(I)})\right| \\ &\quad \le L_{\bar{\eta}_i^{(I)}} \left\|x^{(I)} - \hat{x}^{(I)}\right\|, \quad \forall\, x^{(I)}, \hat{x}^{(I)} \in \mathcal{X}, \end{aligned} \tag{5}$$

where $L_{\bar{\eta}_i^{(I)}}$ indicates the known Lipschitz constant.

The bounds on the modelling uncertainty are needed in order to design the adaptive thresholds, which help to distinguish between the effects of the fault and the modelling uncertainty. The majority of fault diagnosis schemes in the literature consider the modelling uncertainty function $\eta_i^{(I)}$ to be bounded with a known upper-bound function $\bar{\eta}_i^{(I)}$, see Talebi et al. (2009), Wu and Saif (2007), Nemati et al. (2019), Papadopoulos et al. (2017), Boem et al. (2013), T. Chen et al. (2021), Arrichiello et al. (2015), Kougiatsos et al. (2022), X. Zhang and Zhang (2012), X. Zhang (2011) and Keliris et al. (2015b). However, in this work, similar to the Reppa et al. (2014a, 2014b), an unknown but Lipschitz bound function $\bar{\eta}_i^{(I)}$ on the modelling uncertainty function $\eta_i^{(I)}$ is also considered, which is less conservative in practice.

Assumption 2.3: *The measurement noise in the output signal, represented by $\xi_y^{(I)}$, is unknown but uniformly bounded component-wise as follows:*

$$\left|\xi_{y,i}^{(I)}(t)\right| \le \bar{\xi}_{y,i}^{(I)}, \quad i = 1, \ldots, n_I, \tag{6}$$

where $\bar{\xi}_{y,i}^{(I)}$ denotes a known positive constant.

This assumption requires a known bound on the measurement noise which in practice, it can be derived based on the technical specifications of the sensors. This assumption is required in order to be able to distinguish the effects of a fault from the measurement noise, and is commonly used in the fault detection literature (Arrichiello et al., 2015; Boem, Ferrari, Keliris, et al., 2016; Boem, Ferrari, Parisini, 2011; T. Chen et al., 2021; Keliris et al., 2015b; Kougiatsos et al., 2022; Nemati et al., 2019; Papadopoulos et al., 2017; Reppa et al., 2014a, 2014b; Riverso et al., 2016; Talebi et al., 2009; L. Zhang et al., 2020).

In this paper, we consider a distributed actuator fault diagnosis framework, where each subsystem I is monitored by a corresponding FDI agent that receives measurements $y^{(I)}$ from the subsystem it monitors and measurements of the interconnection variables $z^{(I)}$ as $y_z^{(I)}$, communicated by neighbouring detection agents of the Ith subsystem. The detection module of the FDI agent is designed based on the healthy input signal vector $u_H^{(I)}(t)$ of the Ith subsystem which is used for calculating an estimation $\hat{x}_H^{(I)}(t)$ of the states under the healthy mode of operation (based on the healthy system dynamics model), whereas the system is controlled by the fault-prone actuator input $u^{(I)}(t)$. This discrepancy is the basis for the developed actuator fault detection method. The structure of the proposed actuator FDI scheme with the FDI agents containing the actuator fault detection modules and the actuator fault isolation modules is depicted in Figure 1, which considers a system with three-interconnected subsystems. As soon as an actuator fault, within a subsystem, is detected by the actuator fault detection module of its corresponding FDI agent, the actuator fault isolation module is activated to isolate the fault(s). The final decision of the actuator fault detection and isolation modules is a diagnosis set of potential faulty actuators sets.

Remark 2.3: It is important to note that the objective of this work is not to design a feedback control or fault accommodation scheme, but rather to develop methods for detecting and isolating actuator faults in uncertain interconnected nonlinear systems. In practice, the feedback control law may try to 'hide' the fault by reducing its effect on the tracking error. Therefore, a key challenge is to be able to detect and isolate faults despite the presence of robust control schemes.

3. Actuator fault detection

In this section, the problem of multiple actuator fault detection for the class of nonlinear interconnected dynamical systems described by (1) is investigated. Specifically, in this section, we deal with the local actuator fault detection within a subsystem I by designing the residual and corresponding detection thresholds in the fault detection module.

3.1 Residual generation

A residual quantity represents the inconsistency between the estimation model of system variables and their corresponding actual measurements. The estimator corresponding to the nonlinear subsystem I under healthy actuator operation is given as follows:

$$\hat{\Sigma}^{(I)}: \begin{cases} \dot{\hat{x}}^{(I)}(t) = A^{(I)}\hat{x}^{(I)}(t) + g^{(I)}(\hat{x}^{(I)}(t), u_H^{(I)}(t)) \\ \quad +h^{(I)}(\hat{x}^{(I)}(t), y_z^{(I)}(t), u_H^{(I)}(t)) \\ \quad +K^{(I)}\left(y^{(I)}(t) - \hat{y}^{(I)}(t)\right) \\ \hat{y}^{(I)}(t) = \hat{x}^{(I)}(t), \end{cases} \tag{7}$$

where $\hat{x}^{(I)}$ and $\hat{y}^{(I)}$ are the estimations of the state vector $x^{(I)}$ and the output vector $y^{(I)}$ of the Ith subsystem, respectively. The matrix $K^{(I)} \triangleq [k_{ij}^{(I)}]_{n_I \times n_I}$ is a gain matrix which is designed as:

$$K^{(I)} \triangleq A^{(I)} + M^{(I)}, \tag{8}$$

where $M^{(I)}$ is the diagonal matrix $M^{(I)} \triangleq \text{diag}\{\mu_1^{(I)}, \ldots, \mu_{n_I}^{(I)}\}$ where $\mu_i^{(I)}$ are constants selected such that $\mu_i^{(I)} > L_i^{(I)}$ and $L_i^{(I)} \triangleq L_{h_i^{(I)}} + L_{g_i^{(I)}} + L_{\bar{\eta}_i^{(I)}}$, $i = 1, \ldots, n_I$. Note also that the estimator presented in (7) is based on the healthy input vector $u_H^{(I)}$, the local measurement vector $y^{(I)}$ and the communicated measurements $y_z^{(I)}$ from neighbouring FDI agents, constituting the FDI scheme distributed.

The state estimation error $\tilde{x}^{(I)}$ of the Ith subsystem and the output estimation error (residual) $\tilde{y}^{(I)}$ of the Ith subsystem that is used for fault detection are defined respectively as:

$$\tilde{x}^{(I)} \triangleq x^{(I)} - \hat{x}^{(I)}, \tag{9}$$

$$\tilde{y}^{(I)} \triangleq y^{(I)} - \hat{y}^{(I)}. \tag{10}$$

Each component $\tilde{y}_i^{(I)}(t)$ of the residual is compared with an appropriately designed threshold in order to detect the occurrence of a fault. In other words, a system is considered healthy at time t (without fault) if the following inequality is satisfied for all $I \in \{1, \ldots, N\}$ and for all $i \in \{1, \ldots, n_I\}$,

$$\left|\tilde{y}_i^{(I)}(t)\right| \leq \bar{y}_i^{(I)}(t), \tag{11}$$

where $\bar{y}_i^{(I)}(t)$ denotes an adaptive detection threshold (to be designed). If at some time t the residual $\tilde{y}_i^{(I)}(t)$ exceeds its corresponding threshold $\bar{y}_i^{(I)}(t)$ such that inequality (11) is violated, then the existence of a fault in the subsystem I is guaranteed. In the following, the fault occurrence time is defined.

Definition 3.1: The local fault detection time for the Ith subsystem, $T_d^{(I)}$, is defined as

$$T_d^{(I)} = \min\left\{T_{d,1}^{(I)}, \ldots, T_{d,n_I}^{(I)}\right\},$$

where

$$T_{d,i}^{(I)} = \inf\left\{t \,\middle|\, |\tilde{y}_i^{(I)}(t)| > \bar{y}_i^{(I)}(t)\right\}, \quad i = 1, \ldots, n_I.$$

The following indicator function $\varepsilon_i^{(I)}$, which will be used in the sequel, indicates when the ith residual exceeds its corresponding threshold. Specifically, the values $\varepsilon_i^{(I)}(t) = \{-1, +1\}$ indicate that the ith residual has exceeded the corresponding threshold (in absolute value, hence a fault has occurred), whereas $\varepsilon_i^{(I)}(t) = 0$ indicates healthy operation.

$$\varepsilon_i^{(I)}(t) = \begin{cases} +1 & \text{if } \tilde{y}_i^{(I)}(t) > \bar{y}_i^{(I)}(t), \\ -1 & \text{if } \tilde{y}_i^{(I)}(t) < -\bar{y}_i^{(I)}(t), \\ 0 & \text{if } |\tilde{y}_i^{(I)}(t)| < \bar{y}_i^{(I)}(t). \end{cases} \qquad i = 1, \ldots, n_I. \tag{12}$$

Figure 2 illustrates the proposed FDI scheme with more focus on the components of the FDI agent for the Ith subsystem. Note that the information exchanged between the FDI agents is constituted only by the quantities $y_z^{(I)}$ that represent the measurements of the interconnection state variables, i.e. $y_z^{(I)} \triangleq z^{(I)} + \xi_z^{(I)}$ where $\xi_z^{(I)}$ is the measurement noise.

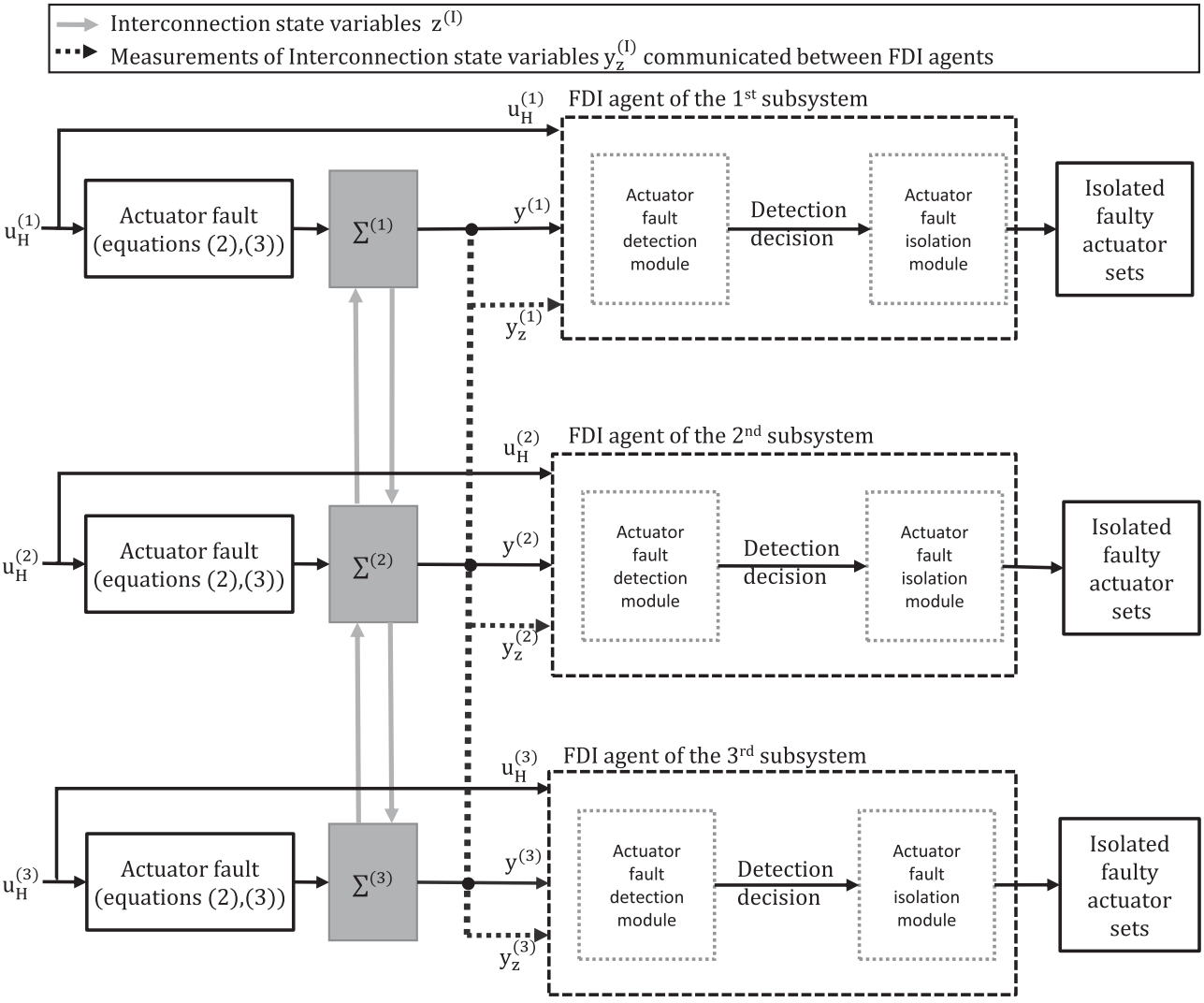

Figure 1. The architecture of the proposed actuator FDI scheme.

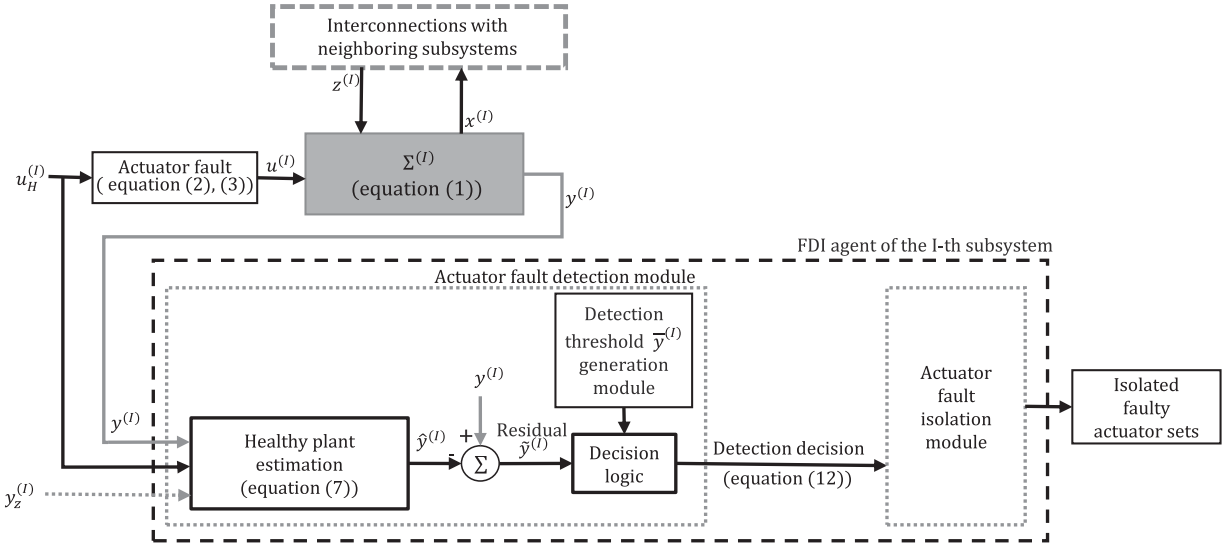

Figure 2. Block diagram of the system modelling and the actuator fault detection agent for the *I*th subsystem. The term $y_z^{(I)}$ is communicated to the *I*th detection agent by neighbouring detection agents.

3.2 Adaptive threshold design

In this part, the problem of local fault estimation for each subsystem is investigated and an adaptive detection threshold is derived. In the following analysis of this section we consider fault free operation, i.e. $t < T_0^{(I)}$, in order to design the detection threshold.

The dynamics of the estimation error system (9) and (10), derived by the subsystem (1) and its estimation in (7) under healthy conditions, i.e. $t < T_0^{(I)}$, are given by

$$\tilde{\Sigma}^{(I)}: \begin{cases} \dot{\tilde{x}}^{(I)}(t) = -M^{(I)}\tilde{x}^{(I)}(t) + g^{(I)}(x^{(I)}(t), u_H^{(I)}(t)) \\ \quad -g^{(I)}(\hat{x}^{(I)}(t), u_H^{(I)}(t)) \\ \quad +h^{(I)}(x^{(I)}(t), z^{(I)}(t), u_H^{(I)}(t))) \\ \quad -h^{(I)}(\hat{x}^{(I)}(t), y_z^{(I)}(t), u_H^{(I)}(t)) \\ \quad +\eta^{(I)}(x^{(I)}(t), z^{(I)}(t), t) - K^{(I)}\xi_y^{(I)}(t) \\ \tilde{y}^{(I)}(t) = \tilde{x}^{(I)}(t) + \xi_y^{(I)}(t). \end{cases} \tag{13}$$

The adaptive detection threshold design is given in the following lemma.

Lemma 3.1: *For the Ith subsystem given in* (1) *and its estimation given in* (7)*, when no faults are present and under Assumptions* 2.1–2.3*, the ith element of the output estimation error* $\tilde{y}^{(I)}$ *given in* (10)*, is uniformly bounded and satisfies*

$$\left|\tilde{y}_i^{(I)}(t)\right| \le \bar{y}_i^{(I)}(t), \quad \forall\, i = 1, \ldots, n_I,\ \forall\, t < T_0^{(I)}, \tag{14}$$

where

$$\bar{y}_i^{(I)}(t) \triangleq \bar{x}_i^{(I)}(t) + \bar{\xi}_{y,i}^{(I)}, \tag{15}$$

$$\bar{x}_i^{(I)}(t) \triangleq f_i^{(I)}(t) + L_i^{(I)} \int_0^t \mathrm{e}^{\left(L_i^{(I)} - \mu_i^{(I)}\right)(t-s)} f_i^{(I)}(s)\, \mathrm{d}s, \tag{16}$$

$$f_i^{(I)}(t) \triangleq \int_0^t \mathrm{e}^{-\mu_i^{(I)}(t-\tau)} \left(\sum_{\substack{j=1 \\ j\neq i}}^{n_I} L_i^{(I)} \bar{x}_j^{(I)}(\tau) + \gamma_i^{(I)} \right) \mathrm{d}\tau + \mathrm{e}^{-\mu_i^{(I)} t} x_0^{(I)}, \tag{17}$$

where $\bar{\xi}_{y,i}^{(I)}$ *is a bound on measurement noise* $\xi_{y,i}^{(I)}$ *defined in* (6)*,* $x_0^{(I)}$ *is a bound on* $|\tilde{x}_i^{(I)}(0)|$*, i.e.* $|\tilde{x}_i^{(I)}(0)| \le x_0^{(I)}$*, and*

$$\gamma_i^{(I)} \triangleq L_{h_i^{(I)}} \bar{\xi}_z^{(I)} + \bar{\eta}_i^{(I)}(\hat{x}^{(I)}, y_z^{(I)}) + |K_i^{(I)} \bar{\xi}_y^{(I)}|. \tag{18}$$

For stability purposes, the elements $\mu_i^{(I)}$ *of the diagonal matrix* $M^{(I)}$ *are selected such that* $\mu_i^{(I)} > L_i^{(I)}$, $i = 1, \ldots, n_I$.

Proof: Under healthy mode of operation, the ith component of $\dot{\tilde{x}}^{(I)}$ given in (13) satisfies

$$\begin{aligned} \dot{\tilde{x}}_i^{(I)} = &-\mu_i^{(I)}\tilde{x}_i^{(I)} + g_i^{(I)}(x^{(I)}, u_H^{(I)}) - g_i^{(I)}(\hat{x}^{(I)}, u_H^{(I)}) \\ &+ h_i^{(I)}(x^{(I)}, z^{(I)}, u_H^{(I)}) - h_i^{(I)}(\hat{x}^{(I)}, y_z^{(I)}, u_H^{(I)}) \\ &+ \eta_i^{(I)}(x^{(I)}, z^{(I)}, t) - K_i^{(I)}\xi_y^{(I)}, \end{aligned} \tag{19}$$

where $K_i^{(I)}$ is the ith row of matrix $K^{(I)}$. By integrating (19), we obtain

$$\begin{aligned} \tilde{x}_i^{(I)} = &\int_0^t \mathrm{e}^{-\mu_i^{(I)}(t-\tau)} \left(g_i^{(I)}(x^{(I)}, u_H^{(I)}) - g_i^{(I)}(\hat{x}^{(I)}, u_H^{(I)}) \right. \\ &+ h_i^{(I)}(x^{(I)}, z^{(I)}, u_H^{(I)}) - h_i^{(I)}(\hat{x}^{(I)}, y_z^{(I)}, u_H^{(I)}) \\ &\left. + \eta_i^{(I)}(x^{(I)}, z^{(I)}, \tau) - K_i^{(I)}\xi_y^{(I)} \right) \mathrm{d}\tau \\ &+ \mathrm{e}^{-\mu_i^{(I)} t}\tilde{x}_i^{(I)}(0). \end{aligned} \tag{20}$$

Then, based on the Lipschitz condition for the functions $g_i^{(I)}$ and $h_i^{(I)}$, the inequality given in (4) of Assumption 2.2 and by using Lemma 2.1, Equation (20) can be written by using the triangle inequality as:

$$\begin{aligned} \left|\tilde{x}_i^{(I)}\right| \le &\int_0^t \mathrm{e}^{-\mu_i^{(I)}(t-\tau)} \left((L_{g_i^{(I)}} + L_{h_i^{(I)}}) \left\|\tilde{x}^{(I)}\right\| \right. \\ &\left. + L_{h_i^{(I)}} \bar{\xi}_z^{(I)} + \bar{\eta}_i^{(I)}(x^{(I)}, y_z^{(I)}) + \left|K_i^{(I)} \bar{\xi}_y^{(I)}\right| \right) \mathrm{d}\tau \\ &+ \mathrm{e}^{-\mu_i^{(I)} t} x_0^{(I)}, \quad \forall\, t < T_0^{(I)}. \end{aligned} \tag{21}$$

Now, for the term $\bar{\eta}_i^{(I)}(x^{(I)}, y_z^{(I)})$, by using the Lipschitz condition given in (5) of Assumption 2.2, and by adding and subtracting $\bar{\eta}_i^{(I)}(\hat{x}^{(I)}, y_z^{(I)})$, we have

$$\begin{aligned} \bar{\eta}_i^{(I)}(x^{(I)}, y_z^{(I)}) &\le \left| \bar{\eta}_i^{(I)}(x^{(I)}, y_z^{(I)}) - \bar{\eta}_i^{(I)}(\hat{x}^{(I)}, y_z^{(I)}) \right. \\ &\quad \left. + \bar{\eta}_i^{(I)}(\hat{x}^{(I)}, y_z^{(I)}) \right| \\ &\le L_{\bar{\eta}_i^{(I)}} \left\|\tilde{x}^{(I)}\right\| + \bar{\eta}_i^{(I)}(\hat{x}^{(I)}, y_z^{(I)}). \end{aligned} \tag{22}$$

Then, by substituting (22) in inequality (21), we obtain

$$\begin{aligned} \left|\tilde{x}_i^{(I)}\right| \le &\int_0^t \mathrm{e}^{-\mu_i^{(I)}(t-\tau)} \left(L_i^{(I)} \left\|\tilde{x}^{(I)}\right\| + \gamma_i^{(I)} \right) \mathrm{d}\tau \\ &+ \mathrm{e}^{-\mu_i^{(I)} t} x_0^{(I)}, \quad \forall\, t < T_0^{(I)}, \end{aligned} \tag{23}$$

where $L_i^{(I)}$ is defined after (8) and, $\gamma_i^{(I)}$ is defined in (18). Furthermore, for the estimation error $\tilde{x}^{(I)} \triangleq [\tilde{x}_1^{(I)}, \tilde{x}_2^{(I)}, \ldots, \tilde{x}_{n_I}^{(I)}]^T$, by using the fact that $\|\tilde{x}^{(I)}\| \le |\tilde{x}_1^{(I)}| + |\tilde{x}_2^{(I)}| + \cdots + |\tilde{x}_{n_I}^{(I)}|$, (which holds for every norm space), therefore, (23) becomes:

$$\begin{aligned} \left|\tilde{x}_i^{(I)}\right| \le &\mathrm{e}^{-\mu_i^{(I)} t} x_0^{(I)} + \int_0^t \mathrm{e}^{-\mu_i^{(I)}(t-\tau)} \\ &\left(\sum_{\substack{j=1 \\ j\neq i}}^{n_I} L_i^{(I)} \left|\tilde{x}_j^{(I)}\right| + L_i^{(I)} \left|\tilde{x}_i^{(I)}\right| + \gamma_i^{(I)} \right) \mathrm{d}\tau, \quad \forall\, t < T_0^{(I)}. \end{aligned} \tag{24}$$

Let $\bar{x}_j^{(I)}(t)$ be a bounding function on $|\tilde{x}_j^{(I)}(t)|$, i.e. $|\tilde{x}_j^{(I)}(t)| \le \bar{x}_j^{(I)}(t)$, $j = 1, \ldots, n_I$, therefore (24) becomes

$$\left|\tilde{x}_i^{(I)}\right| \le \int_0^t L_i^{(I)} \mathrm{e}^{-\mu_i^{(I)}(t-\tau)} \left|\tilde{x}_i^{(I)}\right| d\tau$$

$$+\int_0^t \mathrm{e}^{-\mu_i^{(I)}(t-\tau)}\left(\sum_{\substack{j=1\\ j\neq i}}^{n_I} L_i^{(I)}\bar{x}_j^{(I)}(\tau)+\gamma_i^{(I)}\right)\mathrm{d}\tau$$
$$+\mathrm{e}^{-\mu_i^{(I)}t}x_0^{(I)},\quad \forall\, t<T_0^{(I)}. \tag{25}$$

By applying the Bellman–Gronwall Lemma (Ioannou & Sun, 1996), we obtain

$$\begin{aligned}\left|\tilde{x}_i(t)^{(I)}\right| &\le f_i^{(I)}(t)+L_i^{(I)}\,\mathrm{e}^{-\mu_i^{(I)}(t)}f\\ &\quad\times\int_0^t f_i^{(I)}(s)\,\mathrm{e}^{\mu_i^{(I)}s}\,\mathrm{e}^{\left(\int_s^t \mathrm{e}^{\mu_i^{(I)}\tau}L_i^{(I)}\mathrm{e}^{-\mu_i^{(I)}(\tau)}\,\mathrm{d}\tau\right)}\mathrm{d}s\\ &\le f_i^{(I)}(t)+\int_0^t L_i^{(I)}f_i^{(I)}(s)\,\mathrm{e}^{-\mu_i^{(I)}(t-s)}\,\mathrm{e}^{\int_s^t L_i^{(I)}\,\mathrm{d}\tau}\,\mathrm{d}s\\ &\le \bar{x}_i^{(I)}(t),\quad \forall\, t<T_0^{(I)},\end{aligned} \tag{26}$$

where $f_i^{(I)}(t)$ is defined in (17) and $\bar{x}_i^{(I)}(t)$ is given in (16). As can be seen from (16), for stability it is required that $L_i^{(I)}-\mu_i^{(I)}<0$ and hence, $\mu_i^{(I)}$ must be selected such that $\mu_i^{(I)}>L_i^{(I)}$, $i=1,\ldots,n_I$.

The ith residual of the Ith subsystem can be written based on (10) as follows:

$$\begin{aligned}\tilde{y}_i^{(I)}(t)&=y_i^{(I)}(t)-\hat{y}_i^{(I)}(t)\\ &=\tilde{x}_i^{(I)}(t)+\xi_{y,i}^{(I)}(t),\quad \forall\, i=1,\ldots,n_I,\ \forall\, t<T_0^{(I)}.\end{aligned} \tag{27}$$

By using (6), (26), and by using the triangle inequality, (27) becomes:

$$\begin{aligned}\left|\tilde{y}_i^{(I)}(t)\right| &\le \bar{x}_i^{(I)}(t)\\ &\quad+\bar{\xi}_{y,i}^{(I)}(t)\triangleq\bar{y}_i^{(I)}(t),\quad i=1,\ldots,n_I,\ \forall\, t<T_0^{(I)}.\end{aligned} \tag{28}$$

Therefore, the residual error $\tilde{y}_i^{(I)}(t)$ (under healthy conditions) is bounded by the adaptive threshold $\bar{y}_i^{(I)}(t)$. ■

The component shown in Figure 3 constitutes the detection threshold generation module shown in Figure 2.

If a fault occurs in one of the actuators of the Ith subsystem, the inequality given by (14) may be violated, which indicates the presence of an actuator fault. In other words, a fault in a subsystem can be detected by its corresponding FDI agent given that it creates a sufficiently large discrepancy to the residual so that it exceeds (in absolute value) its corresponding detection threshold. The issue of local fault detectability is discussed in the following subsection.

3.3 Local fault detectability

Fault detectability refers to the derivation of sufficient conditions for the faults so that their detection by the local FDI agent is guaranteed. It is a theoretical result that characterises implicitly the class of actuator faults that can be detected.

The dynamics of the Ith subsystem presented in (1) with some faulty actuators in the Ith subsystem can be written as follows for $t>T_0^{(I)}$ (when at least one actuator fault occurs)

$$\begin{cases}\dot{x}^{(I)}=A^{(I)}x^{(I)}+g^{(I)}\left(x^{(I)},u_H^{(I)}\right)+h^{(I)}\left(x^{(I)},z^{(I)},u_H^{(I)}\right)\\ \qquad\quad+\eta^{(I)}\left(x^{(I)},z^{(I)},t\right)+\Delta\Phi^{(I)}(x^{(I)},z^{(I)},u_H^{(I)},u_f^{(I)})\\ y^{(I)}=x^{(I)}+\xi_y^{(I)},\end{cases} \tag{29}$$

where $u_f^{(I)}$ denotes the control input vector under faulty actuator condition and $\Delta\Phi^{(I)}$ denotes the deviation between the nonlinear terms of $\dot{x}^{(I)}$ given in (1) from their corresponding counterparts in the healthy conditions, due to the effects of the faulty actuators in the dynamics of the Ith subsystem. Specifically, the ith element of the discrepancy $\Delta\Phi^{(I)}$ is given by:

$$\begin{aligned}\Delta\Phi_i^{(I)}(x^{(I)},z^{(I)},u_H^{(I)},u_f^{(I)})&\triangleq g_i^{(I)}(x^{(I)},u_f^{(I)})-g_i^{(I)}(x^{(I)},u_H^{(I)})\\ &\quad+h_i^{(I)}(x^{(I)},z^{(I)},u_f^{(I)})\\ &\quad-h_i^{(I)}(x^{(I)},z^{(I)},u_H^{(I)}).\end{aligned} \tag{30}$$

Considering the dynamic representation of the faulty subsystem (29) and subsystem estimation (7), a sufficient condition for fault detectability is given in the following theorem.

Theorem 3.2 (Local fault detectability): *Consider the local nonlinear subsystem* (1)*, Assumptions* 2.1–2.3*, the residual* $\tilde{y}_i^{(I)}$ *given by* (10)*, and the detection threshold* $\bar{y}_i^{(I)}$ *given in Lemma* 3.1*. Then, an actuator fault in the local subsystem I is guaranteed to be detected by the Ith FDI agent if there exists a time instant* $T_d^{(I)}$ *for which the following inequality holds for some* $i\in\{1,\ldots,n_I\}$

$$\begin{aligned}&\left|\int_{T_0^{(I)}}^{T_d^{(I)}}\mathrm{e}^{-\mu_i^{(I)}(T_d^{(I)}-\tau)}\right.\\ &\quad\left.\times\left[\Delta\Phi_i^{(I)}(x^{(I)}(\tau),z^{(I)}(\tau),u_H^{(I)}(\tau),u_f^{(I)}(\tau))\right]\mathrm{d}\tau\right|\\ &\quad\ge 2\,\bar{y}_i^{(I)}(T_d^{(I)}),\end{aligned} \tag{31}$$

where $\bar{y}_i^{(I)}(t)$ *is given by* (15).

Proof: In a faulty situation, e.g. for $t\ge T_0^{(I)}$, the state estimation error can be obtained based on (29) and the subsystem estimation given in (7) and satisfies:

$$\begin{cases}\dot{\tilde{x}}^{(I)}=\left(A^{(I)}-K^{(I)}\right)\tilde{x}^{(I)}+g^{(I)}\left(x^{(I)},u_H^{(I)}\right)\\ \qquad\quad-g^{(I)}\left(\hat{x}^{(I)},u_H^{(I)}\right)+h^{(I)}\left(x^{(I)},z^{(I)},u_H^{(I)}\right)\\ \qquad\quad-h^{(I)}\left(\hat{x}^{(I)},\hat{z}^{(I)},u_H^{(I)}\right)\\ \qquad\quad+\eta^{(I)}\left(x^{(I)},z^{(I)},t\right)\\ \qquad\quad+\Delta\Phi^{(I)}(x^{(I)},z^{(I)},u_H^{(I)},u_f^{(I)})-K\xi_y^{(I)}\\ \tilde{y}^{(I)}=\tilde{x}^{(I)}+\xi_y^{(I)}.\end{cases} \tag{32}$$

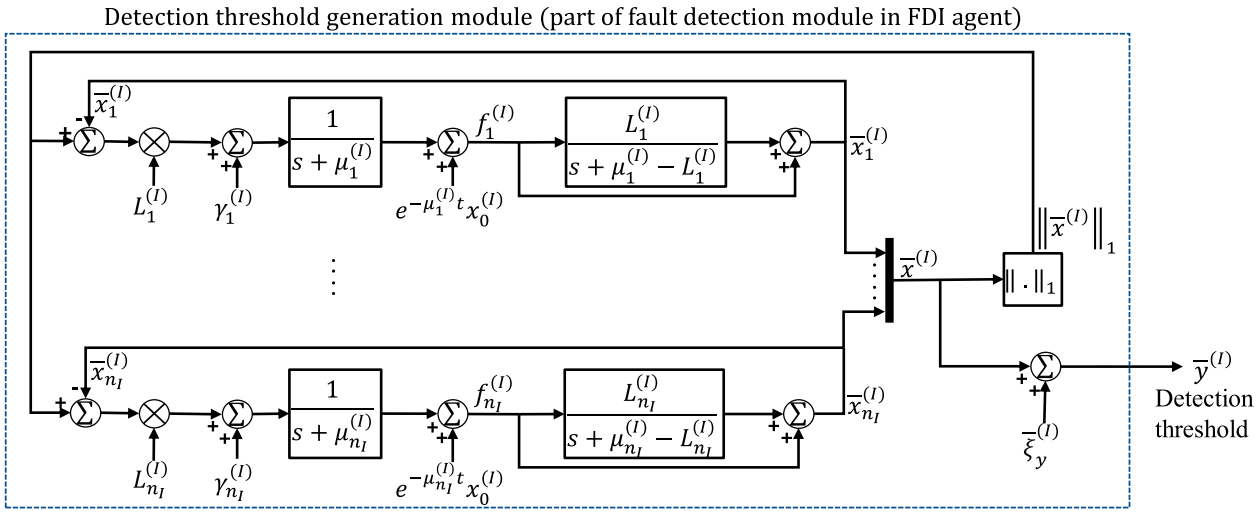

Figure 3. Detection threshold $\bar{y}^{(I)}$ generation by using a novel linear filtering technique.

By integrating the ith element of $\dot{\tilde{x}}^{(I)}$ in (32) and using (8), we obtain:

$$\begin{aligned}\tilde{x}_i^{(I)}(t) = \int_0^t \mathrm{e}^{(-\mu_i^{(I)})(t-\tau)} \Big[& g_i\left(x^{(I)}, u_H^{(I)}\right) - g_i\left(\hat{x}^{(I)}, u_H^{(I)}\right) \\ & + h_i^{(I)}\left(x^{(I)}, z^{(I)}, u_H^{(I)}\right) - h_i^{(I)}\left(\hat{x}^{(I)}, \hat{z}^{(I)}, u_H^{(I)}\right) \\ & + \eta_i^{(I)}\left(x^{(I)}, z^{(I)}, t\right) \\ & + \Delta\Phi_i^{(I)}(x^{(I)}, z^{(I)}, u_H^{(I)}, u_f^{(I)}) - K\xi_y^{(I)}\Big]\,\mathrm{d}\tau \\ & + \mathrm{e}^{-\mu_i^{(I)}t}\tilde{x}_i^{(I)}(0). \end{aligned} \tag{33}$$

By using the inverse triangle inequality, the ith element of $\tilde{y}^{(I)}$ in (32) satisfies

$$\left|\tilde{y}_i^{(I)}(t)\right| \geq \left|\tilde{x}_i^{(I)}(t)\right| - \bar{\xi}_{y,i}^{(I)}(t),$$

and by using (33) with the inverse triangle inequality, we have

$$\begin{aligned}\left|\tilde{y}_i^{(I)}(t)\right| \geq - \Bigg| \int_0^t \mathrm{e}^{-\mu_i^{(I)}(t-\tau)} \Big[& g_i\left(x^{(I)}, u_H^{(I)}\right) - g_i\left(\hat{x}^{(I)}, u_H^{(I)}\right) \\ & + h_i^{(I)}\left(x^{(I)}, z^{(I)}, u_H^{(I)}\right) - h_i^{(I)}\left(\hat{x}^{(I)}, \hat{z}^{(I)}, u_H^{(I)}\right) \\ & + \eta_i^{(I)}\left(x^{(I)}, z^{(I)}, t\right) - K\xi_y^{(I)}\Big]\,\mathrm{d}\tau \Bigg| \\ & + \left| \int_{T_0^{(I)}}^t \mathrm{e}^{-\mu_i^{(I)}(t-\tau)} \left[\Delta\Phi_i^{(I)}(x^{(I)}, z^{(I)}, u_H^{(I)}, u_f^{(I)})\right] \mathrm{d}\tau \right| \\ & - \left|\mathrm{e}^{-\mu_i^{(I)}t}\tilde{x}^{(I)}(0)\right| - \bar{\xi}_{y,i}^{(I)}(t), \end{aligned} \tag{34}$$

considering Assumption 2.3, $\bar{x}_i^{(I)}$ defined in (16), and with a similar derivation process of (26) from (20), inequality (34) becomes

$$\begin{aligned}\left|\tilde{y}_i^{(I)}(t)\right| > & -\bar{x}_i^{(I)}(t) - \bar{\xi}_{y,i}^{(I)}(t) \\ & + \left| \int_{T_0^{(I)}}^t \mathrm{e}^{-\mu_i^{(I)}(t-\tau)} \left[\Delta\Phi_i^{(I)}(x^{(I)}, z^{(I)}, u_H^{(I)}, u_f^{(I)})\right] \mathrm{d}\tau \right| \\ & \geq -\bar{y}_i^{(I)}(t) + \left| \int_{T_0^{(I)}}^t \mathrm{e}^{-\mu_i^{(I)}(t-\tau)} \right. \\ & \left. \times \left[\Delta\Phi_i^{(I)}(x^{(I)}, z^{(I)}, u_H^{(I)}, u_f^{(I)})\right] \mathrm{d}\tau \right|. \end{aligned} \tag{35}$$

For a fault to be detected in the ith residual of the Ith subsystem the condition $|\tilde{y}_i^{(I)}(t)| > \bar{y}_i^{(I)}(t)$ must be satisfied at some time $t = T_d^{(I)}$ and hence, a sufficient condition for this is given by (31). ■

4. Actuator fault propagation

The dynamics of each subsystem are influenced by some states of neighbouring subsystems, through the interconnection terms, thus, a fault in one subsystem can propagate to neighbouring subsystems, in the sense that it may trigger the detection of a fault in a neighbouring subsystem. It is worth mentioning that fault propagation does not mean the creation of new actuator faults in other subsystems as a result of the existence of an actuator fault in one subsystem. Instead, a fault in one subsystem can affect its neighbouring interconnected subsystems behaviour and it is crucial to see whether this fault is detectable by neighbouring fault detection agents or not, something that is the task of this section. In Keliris et al. (2015a), the authors have proved in their setting that process faults, in spite of their effect on other subsystems, cannot be detected by other detection agents. In contrast, sensor faults under uncertain conditions can be detected by their corresponding detection agents or by neighbouring detection agents. In the following, we investigate the actuator fault propagation problem among subsystems. Specifically, in the sequel it is shown that an actuator fault in one subsystem that affects neighbouring subsystems can not be detected by the corresponding agents of these neighbouring subsystems. This is due to the way the estimator (7) is designed.

In the sequel, it is considered that the actuator fault has occurred in the Ith subsystem, and we investigate whether this fault can be detected by the agent of the neighbouring Jth subsystem which is affected by the Ith subsystem through the interconnection terms denoted by the $z^{(J)}$ in the dynamics of the

Jth subsystem. The Jth subsystem model under actuator fault propagation that results from the fault that occurred in some actuators of the Ith subsystem through the interconnection variables $z^{(I)}$ (i.e. $u^{(I)} \neq u_H^{(I)}$) can be presented as follows:

$$\begin{cases} \dot{x}^{(J)} = A^{(J)}x^{(J)} + g^{(J)}(x^{(J)}, u_H^{(J)}) \\ \quad +h^{(J)}(x^{(J)}, z_f^{(J)}, u_H^{(J)}) + \eta^{(J)}(x^{(J)}, z_f^{(J)}, t) \\ y^{(J)} = x^{(J)} + \xi_y^{(J)}, \end{cases} \tag{36}$$

and also its estimation model is given as

$$\begin{cases} \dot{\hat{x}}^{(J)} = A^{(J)}\hat{x}^{(J)} + g^{(J)}(\hat{x}^{(J)}, u_H^{(J)}) \\ \quad +h^{(J)}(\hat{x}^{(J)}, y_{z_f}^{(J)}, u_H^{(J)}) + K^{(J)}(y^{(J)} - \hat{y}^{(J)}), \\ \hat{y}^{(J)} = \hat{x}^{(J)}, \end{cases} \tag{37}$$

where the impact of an actuator fault in the Ith subsystem is contained in the interconnection variables of the Jth subsystem $z^{(J)}$, which is now denoted by the index f, i.e. $z_f^{(J)}$. Accordingly, $y_{z_f}^{(J)} \triangleq z_f^{(J)} + \xi_z^{(J)}$ represents the corresponding measurements of $z_f^{(J)}$, ($\xi_z^{(J)}$ denotes the measurements noise affecting the interconnection variables). Finally, $u_H^{(J)}$ denotes the input of the Jth subsystem, which is considered to be healthy. Therefore, the dynamics of the estimation error of the Jth subsystem which is affected by the Ith actuator faulty vector $u_f^{(I)}$ via the interconnection term $z_f^{(J)}$, can be determined by using (36) and (37) as

$$\begin{cases} \dot{\tilde{x}}^{(J)} = (A^{(J)} - K^{(J)})\tilde{x}^{(J)} + g^{(J)}(x^{(J)}, u_H^{(J)}) - g^{(J)}(\hat{x}^{(J)}, u_H^{(J)}) \\ \qquad + h^{(J)}(x^{(J)}, z_f^{(J)}, u_H^{(J)}) - h^{(J)}(\hat{x}^{(J)}, y_{z_f}^{(J)}, u_H^{(J)}) \\ \qquad + \eta^{(J)}(x^{(J)}, z_f^{(J)}, t) - K^{(J)}\xi_y^{(J)} \\ \tilde{y}^{(J)} = \tilde{x}^{(J)} + \xi_y^{(J)}. \end{cases} \tag{38}$$

Considering the above, the following Lemma summarises the findings for the fault propagation problem. The following result shows that if an FDI agent of a certain subsystem is triggered (i.e. a fault is detected), then the fault is in that specific subsystem (not in any neighbouring interconnected subsystem).

Lemma 4.1 (Isolation of subsystem with faulty actuator(s)): *If an actuator fault in a subsystem I of the model described by* (1)*, then it is guaranteed that the fault will not cause the residual of FDI agents in neighbouring subsystems to exceed their threshold.*

Proof: In order to prove Lemma 4.1, we consider that the Ith actuator vector $u^{(I)}$ is faulty (at least one component) and we need to show that the contaminated residual $\tilde{y}^{(J)}(t)$ of any Jth subsystem that is affected by the Ith subsystem is bounded by its corresponding threshold $\bar{y}^{(J)}(t)$ obtained via Lemma 3.1. When an actuator fault occurs in the Ith subsystem, the states $x^{(I)}$ are contaminated by the fault effects, which are also propagated to subsystem J through the interconnection variables $z_f^{(J)}$. The FDI agent of the Jth subsystem uses the measurements $y_{z_f}^{(J)}$ of the interconnection variables which are also contaminated with the same fault effects (and in addition with measurement noise). Therefore Assumption 2.2 still holds (see Equation (4)). Note that the other Assumptions are still valid by definition. Hence, by following the same analysis as in the proof of Lemma 3.1, we can conclude that the estimation error $\tilde{x}_i^{(J)}$ still satisfies Equations (19)–(25), in which I is substituted with J. Hence, from (25) for the Jth subsystem under fault propagation, we can obtain the following inequality

$$\begin{aligned} \left|\tilde{x}_i^{(J)}\right| \leq \int_0^t L_i^{(J)}\, \mathrm{e}^{-\mu_i^{(J)}(t-\tau)} \left|\tilde{x}_i^{(J)}\right| d\tau + \int_0^t \mathrm{e}^{-\mu_i^{(J)}(t-\tau)} \\ \times \left(\sum_{\substack{j=1 \\ j\neq i}}^{n_J} L_i^{(J)} \bar{\tilde{x}}_j^{(J)}(\tau) + \gamma_i^{(J)} \right) \mathrm{d}\tau \\ + \mathrm{e}^{-\mu_i^{(J)}t} x_0^{(J)}, \quad \forall\, i = 1, \ldots, n_J,\ \forall\, t < T_0^{(J)}. \end{aligned}$$

By applying the Bellman–Gronwall Lemma (Ioannou & Sun, 1996), and by following a similar analysis as applied in the proof of Lemma 3.1, we obtain $|\tilde{x}_i^{(J)}| \leq \bar{\tilde{x}}_i^{(J)}$ where $\bar{\tilde{x}}_i^{(J)}$ is defined in (16) by replacing I with J. Then, similarly to the derivation of (28) we obtain

$$\left|\tilde{y}_i^{(J)}\right| \leq \bar{\tilde{x}}_i^{(J)} + \bar{\tilde{\xi}}_{y,i}^{(J)} = \bar{\tilde{y}}_i^{(J)}, \quad i = 1, \ldots, n_J,$$

which is the detection threshold given in (28). As a result, the actuator fault that occurred in the Ith subsystem does not cause the residual of the FDI agent of the Jth subsystem to exceed its threshold, which implies that an actuator fault that occurs in a subsystem can only be detected by the local FDI agent of its respective subsystem. ■

Remark 4.1: Considering the Assumptions 2.1–2.3, and by following a similar analysis as in the proof of actuator fault propagation given in Lemma 4.1, we can further conclude that a fault that occurs in the actuators of the Ith subsystem cannot affect the residuals that correspond to the states of the Ith subsystem that are not directly affected by the faulty actuators. This essentially means that for a faulty actuator that affects some state equations of subsystem (1) (i.e. the actuator appears explicitly), only the corresponding residuals $\tilde{y}_i^{(I)}(t)$ of these state equations can potentially exceed their threshold. In more detail consider some actuators of the Ith subsystem at time t as faulty, i.e. $u^{(I)}(t) \neq u_H^{(I)}(t)$. Assume that the jth state of the Ith subsystem, i.e. $x_j^{(I)}$, $j \in \{1, \ldots, n_I\}$ is a state that is not affected directly by the faulty actuators of the Ith subsystem. Then, it is guaranteed that no fault can be detected in the jth residual of the Ith subsystem, i.e. it is guaranteed that $|\tilde{y}_j^{(I)}(t)| \leq \bar{\tilde{y}}_j^{(I)}(t)$, $\forall\, t \geq 0$, even though a fault is present in the Ith subsystem. Essentially, this is because $\Delta\Phi_j^{(I)}(t) = 0\ \forall\, t \geq 0$, in this case.

5. Actuator fault isolation

Upon the detection of a fault in a subsystem by the fault detection module of the FDI agent, the isolation module of the FDI agent is then initiated to conduct a further analysis in order to narrow down the set of potential faulty actuator(s) as far as possible or even pinpoint exactly which actuators are faulty. Hence,

the task in this Section is to design a process based on a decision logic algorithm which requires the computation of one or several fault hypotheses, based on the residual outputs, where a fault hypothesis is considered to be a set of faults that comply with the observed residual output behaviour (i.e. whether the residuals exceed their corresponding thresholds as indicated by Remark 4.1), Jung et al. (2015).

A. Fault Isolation Strategy

In the fault propagation section, it has been proved that a fault in one subsystem cannot trigger a detection agent in a neighbouring subsystem. Therefore, we only need to consider local fault isolation, and thus, when an actuator fault is detected in the Ith subsystem, it is sufficient to initiate only the isolation agent contained in the same FDI agent (of the Ith subsystem) to isolate the faulty actuators. To this end, the observed pattern of the actuator fault vector $\mathcal{E}^{(I)}(t) \triangleq [\varepsilon_1^{(I)}(t), \ldots, \varepsilon_{n_I}^{(I)}(t)]^T$, which is now nonzero since a fault is detected (i.e. see Equation (12)), is utilised to make a decision about the diagnosis sets of faulty actuators $\mathcal{D}_s^{(I)}(t)$ and $\mathcal{D}_w^{(I)}(t)$ among the global actuator fault sets $\mathcal{F}^{(I)} = \{\mathcal{F}_{c_i}^{(I)} \mid \forall\, i = 1, \ldots, 2^{m_I} - 1\}$, where $\mathcal{F}_{c_i}^{(I)}$ is a set of all possible faulty actuator combinations of the Ith subsystem, i.e. $\mathcal{D}_s^{(I)}(t), \mathcal{D}_w^{(I)}(t) \subseteq \mathcal{F}^{(I)}$. $\mathcal{D}_s^{(I)}(t)$ presents the potential faulty actuator sets and $\mathcal{D}_w^{(I)}(t)$ is the weakly faulty actuator sets which will be discussed in the sequel. Specifically, the goal of this section is to find these diagnosis sets of the 'suspected' faulty actuator sets of the Ith subsystem. $\mathcal{E}^{(I)}(t) \neq 0_{n_I}$ means that a fault has been detected in the Ith subsystem. Hence, when $\mathcal{E}^{(I)}(t) \neq 0_{n_I}$, the fault isolation module of the Ith FDI agent is activated to isolate the possible faulty actuators of the Ith subsystem.

In Remark 2.1, it has been stated that the faulty actuator(s) are contained within the state equations $\dot{x}_i^{(I)}$ for which the corresponding residuals $\tilde{y}_i^{(I)}$ exceed (in absolute value) their threshold $\bar{y}_i^{(I)}$. Therefore, in the actuator fault isolation process, we can use this information for the construction of the signature matrix,

$$F^{(I)} = \left[F_{ij}^{(I)}\right]_{n_I \times |\mathcal{F}^{(I)}|}, \tag{39}$$

where $\mathcal{F}^{(I)}$, as stated earlier, is a set that contains all possible combinations of actuator sets. Thus, $|\mathcal{F}^{(I)}|$ denotes the cardinality of the actuator combination set $\mathcal{F}^{(I)}$ which is equal to $2^{m_I} - 1$. It is worth mentioning that, in the case of a single actuator fault occurrence, the cardinality of the actuator combination set $\mathcal{F}^{(I)}$ would be m_I, i.e. $\mathcal{F}^{(I)} = \{\{u_1^{(I)}\}, \ldots, \{u_{m_I}^{(I)}\}\}$.

Each column j of the signature matrix $F^{(I)}$ (in the sequel it will be denoted as $F_j^{(I)}$) is linked with the fault set $\mathcal{F}_{c_j}^{(I)}$ and each element i of $F_j^{(I)}$ denotes the potential effect of the fault in the actuator combination set $\mathcal{F}_{c_j}^{(I)}$ on the residual $\tilde{y}_i^{(I)}$, i.e. $\varepsilon_i^{(I)}(t)$ (see (12)). Therefore, the signature matrix $F^{(I)}$ is used to isolate the fault(s) by comparing its columns with the observed pattern of actuator faults vector $\mathcal{E}^{(I)}(t)$.

The entry $F_{ij}^{(I)}$, which indicates the potential effect of the fault in the jth actuator combination set $\mathcal{F}_{c_j}^{(I)}$ (all actuators in $\mathcal{F}_{c_j}^{(I)}$ are considered faulty) on the behaviour of the ith residual $\tilde{y}_i^{(I)}(t)$ of the Ith subsystem is calculated as follows:

(1) $F_{ij}^{(I)} = 0$, if the fault in the actuator combination set $\mathcal{F}_{c_j}^{(I)}$ has no effect on the residual $\tilde{y}_i^{(I)}$ with respect to its value in healthy mode of operation. For example, this occurs when the $\mathcal{F}_{c_j}^{(I)}$ does not affect $\dot{x}_i^{(I)}$ directly (hence none of the actuators of the actuator combination set $\mathcal{F}_{c_j}^{(I)}$ appears in the equation of $\dot{x}_i^{(I)}$).

(2) $F_{ij}^{(I)} = -1$, if the fault in the actuator combination set $\mathcal{F}_{c_j}^{(I)}$ causes the decrease of the residual $\tilde{y}_i^{(I)}$ with respect to its value in healthy mode of operation. For instance, this can happen when all actuators in $\mathcal{F}_{c_j}^{(I)}$ have positive sign and are simply added in the equation $\dot{x}_i^{(I)}(t)$ (i.e. $\dot{x}_1 = x_1 + u_1,\ u_1 > 0$).

(3) $F_{ij}^{(I)} = +1$, if the fault in the actuator combination set $\mathcal{F}_{c_j}^{(I)}$ causes the increase of the residual $\tilde{y}_i^{(I)}$ with respect to its value in healthy mode of operation. For instance, this can happen when all the actuators in $\mathcal{F}_{c_j}^{(I)}$ have positive sign and are simply subtracted in the equation $\dot{x}_i^{(I)}(t)$ (i.e. $\dot{x}_1 = x_1 - u_1,\ u_1 > 0$).

(4) $F_{ij}^{(I)} = *$, if the fault in the actuator combination set $\mathcal{F}_{c_j}^{(I)}$ affects the residual $\tilde{y}_i^{(I)}$ but, it is not certain if it increases or decreases its value. For example, this may happen when some actuators in $\mathcal{F}_{c_j}^{(I)}$ have positive effect on $\dot{x}_i^{(I)}(t)$ but the rest have negative effect on $\dot{x}_i^{(I)}(t)$ (i.e. $\dot{x}_1 = x_1 + u_1 - u_2,\ u_1, u_2 > 0$).

Remark 5.1: Although the proposed method in this paper considers only multiplicative faults as defined in (2), it is important to note that the proposed approach works for any type of actuator faults, i.e. additive faults. However, by considering other actuator fault types rather than multiplicative faults, the decreasing or increasing effect of such faults on their corresponding actuators values cannot be specified and as a result, the signature matrix (39) can only be bi-valued, i.e. $F_{ij}^{(I)} \in \{0, *\}$.

In the following, an example is given to clarify the above and to explain how the signature matrix $F^{(I)}$ elements are determined.

Example 5.1: Consider the dynamical system

$$\begin{cases} \dot{x}_1 = f_1(x_1, x_2, x_3) + u_1 - u_3 \\ \dot{x}_2 = f_2(x_1, x_2, x_3) + u_2 - x_1 u_1 \\ \dot{x}_3 = f_3(x_1, x_2, x_3) + u_3 \\ y_i = x_i + \xi_{y,i} \quad i = 1, 2, 3, \end{cases} \tag{40}$$

where f_1, f_2 and f_3 are some functions. For the example, assume that the signs of the values of all the actuator inputs are positive (i.e. so that u_1 is positive and $-u_3$ is negative). It is worth noting that the designed scheme can be utilised in systems with undefined actuator signs (see Remark 5.1). The signature matrix related to the dynamical system (40), relates each fault set with

each residual. It is worth mentioning that, the signature matrix elements are obtained by considering the decreasing effect that a fault has on the actuator values (in absolute value – recall (2), (3) which indicate loss of performance of actuators). For example, a fault in actuator u_1 (considering u_1 is positive), has negative effect on the value of residual $\tilde{y}_1$, in other words it reduces the value of $\tilde{y}_1$. Therefore, we set $F_{1,1} = -1$. Also, the effect of a fault in actuator u_1 can result in increase or decrease of the value of the residual $\tilde{y}_2$, since its coefficient x_1 in equation $\dot{x}_2$ has an undefined sign. Therefore, we set $F_{2,1} = *$. The actuator u_1 does not have any direct effect on the value of residual $\tilde{y}_3$ since it does not appear in the state equation of $\dot{x}_3$. Therefore, we set $F_{3,1} = 0$. In order to quantify the signature matrix F, this process is done for each fault combination set $\mathcal{F}_{c_j}$ and determine how each set affects each residual. Finally, the signature matrix can be obtained as follows

$$F = \begin{array}{c} \begin{matrix} \mathcal{F}_{c_1} & \mathcal{F}_{c_2} & \mathcal{F}_{c_3} & \mathcal{F}_{c_4} & \mathcal{F}_{c_5} & \mathcal{F}_{c_6} & \mathcal{F}_{c_7} \end{matrix} \\ \begin{pmatrix} -1 & 0 & +1 & -1 & * & +1 & * \\ * & -1 & 0 & * & * & -1 & * \\ 0 & 0 & -1 & 0 & -1 & -1 & -1 \end{pmatrix} \end{array} \begin{matrix} \\ \rightarrow \tilde{y}_1 \\ \rightarrow \tilde{y}_2 \\ \rightarrow \tilde{y}_3 \end{matrix} \tag{41}$$

where $\mathcal{F}_{c_1} = \{u_1\}, \mathcal{F}_{c_2} = \{u_2\}, \mathcal{F}_{c_3} = \{u_3\}, \mathcal{F}_{c_4} = \{u_1, u_2\}$, $\mathcal{F}_{c_5} = \{u_1, u_3\}, \mathcal{F}_{c_6} = \{u_2, u_3\}$, and $\mathcal{F}_{c_7} = \{u_1, u_2, u_3\}$ are the respective fault combination sets related to all columns of the signature matrix F (column F_j is the fault signature of the fault set $\mathcal{F}_{c_j}$).

In the following, some definitions are given.

Definition 5.1: Fault sets $\mathcal{F}^{(I)}_{c_i}, \mathcal{F}^{(I)}_{c_j} \in \mathcal{F}^{(I)}$ are weakly isolable if their corresponding fault signatures $F^{(I)}_i$ and $F^{(I)}_j$ are different.

It is worth mentioning that sometimes, due to the different sensitivity of residuals, some residual signals violate earlier their corresponding thresholds than other residuals, which results in a signature match with a different fault set than the actual one. Thus, weak isolability cannot guarantee the derivation of the correct faulty actuators set (Edwards et al., 2000). For example (in the case of Example 5.1), consider $F_1 = [-1 \ *0]^T$ and $F_2 = [0 \ -1 \ 0]^T$ given in (41) which are the signatures of fault sets $\mathcal{F}_{c_1} = \{u_1\}$ and $\mathcal{F}_{c_2} = \{u_2\}$, respectively. The Fault sets $\mathcal{F}_{c_1}, \mathcal{F}_{c_2}$ are weakly isolable. Now, assume that only actuator $u_1(t)$ (at time t) is faulty and the observed pattern of the fault at time t is $\mathcal{E}(t) = [0 \ -1 \ 0]^T$. Then, the diagnosed fault set at time t is determined to be $\mathcal{F}_{c_2} = \{u_2\}$, which is not correct. At some time t, it is reasonable to expect to have the observed fault pattern $\mathcal{E}(t) = [-1 \ * \ 0]^T$ so that the diagnosed fault set is $\mathcal{F}_{c_1} = \{u_1\}$ but this is not guaranteed that it will be observed. In this example, this can happen due to the effects of x_1 as the coefficient of u_1 that happens to amplify the fault effect on $\dot{x}_2$. As a result, the residual $\tilde{y}_2$ can violate earlier than the residual $\tilde{y}_1$ its corresponding threshold.

Definition 5.2 (Huang et al., 2000)**:** Fault sets $\mathcal{F}^{(I)}_{c_i}, \mathcal{F}^{(I)}_{c_j} \in \mathcal{F}^{(I)}$ are strongly isolable if their corresponding signatures $F^{(I)}_i$ and $F^{(I)}_j$ are different and also, the fault signature $F^{(I)}_i$ can not be obtained from the fault signature $F^{(I)}_j$ by turning some non-zero elements in $F^{(I)}_j$ into zeros; and vice versa.

Table 1. Strong inconsistency cases, $i \in \{1, \ldots, m_I\}$ and $k \in \{1, \ldots, 2^{m_I} - 1\}$.

$\varepsilon^{(I)}_i(t)$	$F^{(I)}_{ik}$
$+1$	0
$+1$	-1
-1	0
-1	$+1$

In this paper, when $F^{(I)}_{ik} = *$ and $F^{(I)}_{jk} = \pm 1$, $k \in \{1, \ldots, n_I\}$, the position of the $*$ element is ignored. For example, $F_i = [-1 \ * \ 0]^T$ and $F_j = [0 \ +1 \ 0]^T$ are not strongly isolable, i.e. F_j can be obtained from the fault signature F_i by turning F_{i1} from its value '-1' to zero.

The problem is that in many large-scale systems, only a few cases are strongly isolable. As a result, in some fault isolation cases, isolating the correct fault set becomes impossible.

In the sequel, the strong inconsistency between the pattern of the observed actuator fault vector $\mathcal{E}^{(I)}(t)$ and the signature pattern of fault set $\mathcal{F}^{(I)}_{c_j}$, i.e. $F^{(I)}_j$ is defined.

Definition 5.3: The signature pattern of the fault set $\mathcal{F}^{(I)}_{c_j} \in \mathcal{F}^{(I)}$ has strong inconsistency with the observed pattern of the fault vector $\mathcal{E}^{(I)}(t)$, if the observed pattern of the fault vector $\mathcal{E}^{(I)}(t)$ shows a fault in at least one of its elements, whereas the signature pattern of $\mathcal{F}^{(I)}_{c_j}$ does not indicate that type of fault or does not have a fault, i.e. the respective elements are zero. The strong inconsistency between the observed pattern of the actuator fault $\mathcal{E}^{(I)}(t)$ and the fault set $\mathcal{F}^{(I)}_{c_k}$, $k \in \{1, \ldots, 2^{m_I - 1}\}$ is defined as follows

$$\varepsilon^{(I)}_i(t) \neq F^{(I)}_{ik}, \quad \text{for some } i \in \mathcal{J}^{(I)}, \tag{42}$$

where $\mathcal{J}^{(I)} = \{j \,|\, |\tilde{y}^{(I)}_j| > \bar{y}^{(I)}_j\}$. When $F^{(I)}_{ik} = *$ condition (42) is ignored for the ith element.

Strong inconsistency is important in the fault isolation process and in Table 1, all the cases of strong inconsistencies are given.

The consistency between a fault set $\mathcal{F}^{(I)}_{c_k}$ and the pattern of the observed actuator fault set $\mathcal{E}^{(I)}(t)$ occurs when

$$\begin{cases} \varepsilon^{(I)}_i(t) = F^{(I)}_{ik} \text{ or } F^{(I)}_{ik} = * & \forall\, i \in \mathcal{J}^{(I)} \\ F^{(I)}_{ik} = 0 & \forall\, i \notin \mathcal{J}^{(I)}, \end{cases} \tag{43}$$

where $\mathcal{J}^{(I)} = \{j \,|\, |\tilde{y}^{(I)}_j| > \bar{y}^{(I)}_j\}$. If there is a consistency between a fault set $\mathcal{F}^{(I)}_{c_k}$ and the pattern of the observed actuator fault vector $\mathcal{E}^{(I)}(t)$, $\mathcal{F}^{(I)}_{c_k}$ is considered as one suspect set of the faulty sets, i.e. $\mathcal{F}^{(I)}_{c_k} \in \mathcal{D}^{(I)}_s(t)$, where $\mathcal{D}^{(I)}_s(t)$ denotes the diagnosis set of faulty actuators sets, that is, it contains the potential faulty

actuator sets. In fact, the diagnosis set $\mathcal{D}_s^{(I)}(t)$ contains the actuator fault sets that are consistent with the pattern of the observed fault vector $\mathcal{E}^{(I)}(t)$,

$$\mathcal{D}_s^{(I)}(t) \triangleq \left\{ \mathcal{F}_{c_k}^{(I)} \middle| \mathcal{F}_{c_k}^{(I)} \text{ satisfies (43), where } k \in \{1, \ldots, 2^{m_I} - 1\} \right\}. \quad (44)$$

It must be noted that, based on the fault magnitude (actuator performance loss), sometimes the signature matrix of an actuator fault set $\mathcal{F}_{c_k}^{(I)}$ cannot be matched in all its residuals, i.e. for a column $k \in \{1, \ldots, 2^{m_I} - 1\}$, $F_{ik}^{(I)} \neq 0$ whereas $\varepsilon_i^{(I)}(t) = 0$ for some $i \in \{1, \ldots, n_I\}$. This means that there is no consistency between the fault set $\mathcal{F}_{c_k}^{(I)}$ and the detected pattern of the observed fault vector $\mathcal{E}^{(I)}(t)$. The problem occurs when all sets of faults $\mathcal{F}_{c_k}^{(I)}$, $k = 1, \ldots, 2^{m_I} - 1$ are not consistent with the observed pattern of $\mathcal{E}^{(I)}(t)$ and therefore, the diagnosis set $D_s^{(I)}(t)$ is empty or even sometimes contains erroneous fault sets due to the weak isolability between the erroneous fault sets and the actual faulty actuator set. To deal with this problem, the actuator fault combinations, involved in the violated analytical redundancy relations (ARRs) (Cordier et al., 2004), is utilised, i.e.

$$\mathcal{D}_w^{(I)}(t) = \left\{ \mathcal{F}_{c_k}^{(I)} \middle| \varepsilon_j^{(I)}(t) = F_{jk}^{(I)}, \forall j \in \mathcal{J}^{(I)}, \text{ where } k \in \{1, \ldots, 2^{m_I} - 1\} \right\}. \quad (45)$$

Note that, the case of $F_{ik}^{(I)} = *$ are not included in (45). $\mathcal{D}_w^{(I)}(t)$ provides a weakly consistent set of actuator faults combinations that are involved in the violated ARRs. It is important to note that, comparing (44) and (45), it results that $\mathcal{D}_s^{(I)}(t) \subseteq \mathcal{D}_w^{(I)}(t)$, $\forall\, t \geq 0$, that is, the consistency condition in the derivation of the actuator fault set $\mathcal{D}_s^{(I)}(t)$, due to more restrictions, provides a smaller (or equal) number of diagnosed potential actuator fault combinations compared to the actuator fault combinations $\mathcal{D}_w^{(I)}(t)$ involved in the violated ARRs. Although the diagnosis set $\mathcal{D}_s^{(I)}(t)$ is not guaranteed to contain the actual faulty actuator set, but, it contains more probable faulty actuator combination sets than the fault combination sets contained in $\mathcal{D}_w^{(I)}(t)$ that are determined based on the weakly consistency condition.

Remark 5.2: The weakly consistent diagnosis set $\mathcal{D}_w^{(I)}(t)$ contains the actual faulty actuators set. In other words, assume that $\mathcal{F}_{c_r}^{(I)}$ for some $r \in \{1, \ldots, 2^{m_I} - 1\}$ is the actual actuators fault set at time t. Then, it is clear that, when the jth residual $\tilde{y}_j^{(I)}$ violates its corresponding threshold as a result of a fault in $\mathcal{F}_{c_r}^{(I)}$, i.e. $\varepsilon_j^{(I)}(t) \neq 0$, we have $\varepsilon_j^{(I)}(t) = F_{jr}^{(I)}$ or $F_{jr}^{(I)} = *$ for all $j \in \{1, \ldots, n_I\}$. Therefore, $\mathcal{F}_{c_r}^{(I)} \in \mathcal{D}_w^{(I)}(t)$. A direct result of this is that $\mathcal{F}_w^{(I)} \triangleq \bigcap_{i=1}^{2^{m_I}-1} \{\mathcal{F}_{c_i}^{(I)} | \mathcal{F}_{c_i}^{(I)} \in \mathcal{D}_w^{(I)}(t)\} \subseteq \mathcal{F}_{c_r}^{(I)}$ which indicates that the actuators that belong to the set $\mathcal{F}_w^{(I)}(t)$ are always correctly identified as faulty. It means that, for all $j \in \{1, \ldots, m_I\}$ such that $u_j^{(I)} \in \mathcal{F}_w^{(I)}(t)$, we have $u_j^{(I)} \in \mathcal{F}_{c_r}^{(I)}$. However $\mathcal{F}_w^{(I)}$ may not contain all the faulty actuators, i.e. $\mathcal{F}_w^{(I)} \subseteq \mathcal{F}_{c_r}^{(I)}$

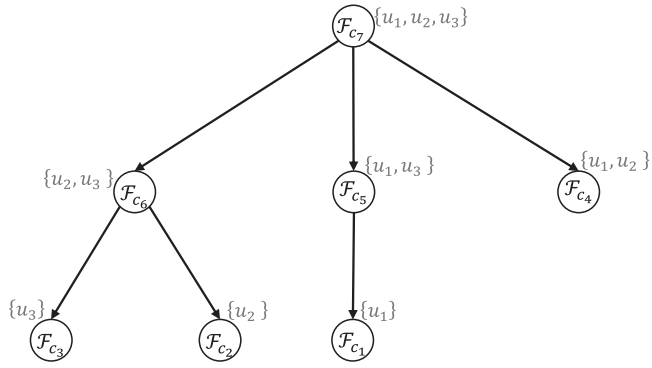

Figure 4. Block diagram of the ISE-tree for a system with 3 actuators and all possible fault sets $\mathcal{F}_{c_i}^{(I)}$, $i = 1, 2, \ldots, 7$.

B. Fault Isolation Implementation

In large-scale systems with a large number of actuators, the size of the actuator fault combination set $\mathcal{F}^{(I)}$ increases exponentially (note that the cardinality of $\mathcal{F}^{(I)}$ is $2^{m_I} - 1$). As a result, the size of the signature matrix $F^{(I)}$, i.e. $n_I \times (2^{m_I} - 1)$, increases significantly. Consequently, the number of searches that need to be made to find potential column matches of the matrix $F^{(I)}$ with $\mathcal{E}^{(I)}(t)$ at every time instant grows exponentially. Thus, the main drawback of using a signature matrix for fault isolation is the computational complexity that makes it inappropriate for use especially in the case of systems containing several possibly faulty actuators (Bartys, 2015b).

To this end, decision trees, as an underlying framework for conducting searches, are used by many learning algorithms (Rymon, 1993). In Zhao and Ouyang (2007), the structure of Set Enumeration (SE) tree along with some implementation algorithm of inverse SE-tree (ISE-tree) is given in detail.

In this paper, the isolation search problem is solved by designing an algorithm based on the ISE-tree. An ISE-tree representation of the faults set must embed all the fault set $\mathcal{F}^{(I)}$ elements in a way such that each fault combination set is assigned to only one node of the ISE-tree. In ISE-tree representation of faults, every possible set of faults has exactly one path from the root of the ISE-tree, along which it can be classified. A typical example of the structure of the ISE-tree of a system containing three actuators is given in Figure 4. As it can be seen, each root is assigned the superior set of actuators with respect to the nodes of its branch. This type of representation helps in conducting efficient searching as is discussed in the following Remark.

Remark 5.3: In ISE-tree evaluation, when a node with label $\mathcal{F}_{c_k}^{(I)}$ $k \in \{1, \ldots, 2^{m_I} - 1\}$ is reached such that $\mathcal{F}_{c_k}^{(I)}$ has strong inconsistency with $\mathcal{E}^{(I)}(t)$, since all its children (which are subsets of $\mathcal{F}_{c_k}^{(I)}$) have strong inconsistency with $\mathcal{E}^{(I)}(t)$, then there is no need to proceed along the branch of the tree from that node. Therefore, by using the strong inconsistency concept, the time complexity of the isolation process can be reduced.

Note that if a fault set $\mathcal{F}_{c_k}^{(I)}$ $k \in \{1, \ldots, 2^{m_I} - 1\}$ does not have strong inconsistency with $\mathcal{E}^{(I)}(t)$, then its subsets may or may not have strong inconsistency.

C. Summary of diagnostic logic

In summary, the intersection set $\mathcal{F}_w^{(I)} = \bigcap_{i=1}^{2^{m_I}-1}\{\mathcal{F}_{c_i}^{(I)} | \mathcal{F}_{c_i}^{(I)} \in \mathcal{D}_w^{(I)}(t)\}$ always contains correctly diagnosed faulty actuators, but, it may not contain all the faulty actuators or it may even contain none of them. On the other hand, the weakly consistent set $\mathcal{D}_w^{(I)}(t)$, which is based on the weakly consistency condition in (45), contains always the actual faulty actuators set. However, the potential fault diagnosis set $\mathcal{D}_s^{(I)}(t)$ which is obtained based on consistency condition in (43), can provide fewer (or at most the same) and more probable faulty actuator sets than $\mathcal{D}_w^{(I)}(t)$ but, there is the risk that the actual faulty actuator set is not included in $\mathcal{D}_s^{(I)}(t)$. As a result, the actuator fault isolation module proposed in this paper returns $\mathcal{D}_s^{(I)}(t)$, $\mathcal{D}_w^{(I)}(t)$ and $\mathcal{F}_w^{(I)}(t)$ based on which, the system operator can infer some information about which actuators are definitely faulty and which might also be faulty.

Algorithm 1 Fault isolation procedure using designed ISE-tree based method

Output: $\mathcal{D}_s^{(I)}$ and $\mathcal{D}_w^{(I)}$: The sets containing the consistent and weakly consistent diagnosed sets of faulty actuators, respectively.

Initialise: $\mathcal{D}_s^{(I)} = \{\}$, $\mathcal{D}_w^{(I)} = \{\}$, $\mathcal{F}_{c_k}^{(I)} = \{u_1^{(I)}, \cdots, u_{m_I}^{(I)}\}$, *node#* $= 0$, % *node#* : node number,

function $[\mathcal{D}_s^{(I)}, \mathcal{D}_w^{(I)}]$ =SE_tree $(\mathcal{D}_s^{(I)}, \mathcal{D}_w^{(I)}, \mathcal{F}_{c_k}^{(I)}, node\#)$

  if $\mathcal{F}_{c_k}^{(I)}$ is strongly inconsistent with $\mathcal{E}^{(I)}(t)$ **then** % Equation (42)

    return

  end if

  if $\mathcal{F}_{c_k}^{(I)}$ is consistent with $\mathcal{E}^{(I)}(t)$ **then** % using Equation (43)

    $\mathcal{D}_s^{(I)} = \mathcal{D}_s^{(I)} \cup \mathcal{F}_{c_k}^{(I)}$

  end if

  if $\mathcal{F}_{c_k}^{(I)}$ is weakly consistent with $\mathcal{E}^{(I)}(t)$ **then** % using Equation (45)

    $\mathcal{D}_w^{(I)} = \mathcal{D}_w^{(I)} \cup \mathcal{F}_{c_k}^{(I)}$

  end if

  LOOP Process

  for each $i = node\#$ to m_I %for each child of *node#*

    $\mathcal{F}_{c_k,i}^{(I)} = \mathcal{F}_{c_k}^{(I)} - \{u_i^{(I)}\}$

    if $\mathcal{F}_{c_k,i}^{(I)} \neq \{\}$ **then**

      $[\mathcal{D}, \mathcal{W}]$ = SE_tree $(\mathcal{D}_s^{(I)}, \mathcal{D}_w^{(I)}, \mathcal{F}_{c_k,i}^{(I)}, i)$

      $\mathcal{D}_s^{(I)} = \mathcal{D}_s^{(I)} \cup \mathcal{D}$

      $\mathcal{D}_w^{(I)} = \mathcal{D}_w^{(I)} \cup \mathcal{W}$

    end if

  end for

  return

In the sequel, the implementation of the fault isolation approach is explained by continuing the Example 5.1 that considers the dynamical system given in (40) and its signature matrix given in (41) which is calculated by considering that the system actuators are positive, i.e. $u_i > 0, \imath = 1, 2, 3$. Considering the system (40) and also by assuming that the observed pattern of the actuator fault detection at time t is $\mathcal{E}(t) = [-1 \ -1 \ 0]^T$, the process of Algorithm 1 for obtaining the diagnosis fault sets $\mathcal{D}_s(t)$ and $\mathcal{D}_w(t)$ is described as follows: Algorithm 1 receives the set $\mathcal{F}_{c_7} = \{u_1, u_2, u_3\}$ as the input argument. Then by evaluating the consistency of $\mathcal{F}_{c_7}$ with the observed pattern of the fault vector $\mathcal{E}(t)$, it results that it is not consistent and hence $\mathcal{F}_{c_7}$ will not be considered as a member of the diagnosis fault set $\mathcal{D}_s(t)$. In addition $\mathcal{F}_{c_7}$ is considered as a member of the weakly diagnosis set $\mathcal{D}_w(t)$ since it is weakly consistent with $\mathcal{E}(t)$. Then, based on the loop process in Algorithm 1, the algorithm will be iterated for each child of $\mathcal{F}_{c_7}$ name as $\mathcal{F}_{c_6}, \mathcal{F}_{c_5}$ and $\mathcal{F}_{c_4}$ and so on (see Figure 4). It is worth mentioning that in the iteration of Algorithm 1 for the fault set $\mathcal{F}_{c_6}$, due to the strong inconsistency of $\mathcal{F}_{c_6}$ with the observed pattern of fault $\mathcal{E}(t)$, the evaluation of Algorithm 1 for all the descendants of $\mathcal{F}_{c_6}$, i.e. $\mathcal{F}_{c_2} = \{u_2\}$ and $\mathcal{F}_{c_3} = \{u_3\}$ is not conducted (hence skipped). Finally, the diagnosis fault sets are obtained as

$$\begin{aligned}\mathcal{D}_s &= \left\{\mathcal{F}_{c_1}, \mathcal{F}_{c_4}\right\} = \{\{u_1\}, \{u_1, u_2\}\}, \\ \mathcal{D}_w &= \left\{\mathcal{F}_{c_1}, \mathcal{F}_{c_4}, \mathcal{F}_{c_5}, \mathcal{F}_{c_7}\right\} \\ &= \{\{u_1\}, \{u_1, u_2\}, \{u_1, u_3\}, \{u_1, u_2, u_3\}\},\end{aligned}$$

and hence, the intersection set $\mathcal{F}_w(t) = \{u_1\}$, which declares that u_1 is correctly identified as a faulty actuator. It is worth mentioning that since the fault sets $\mathcal{F}_{c_5} = \{u_1, u_3\}$, and $\mathcal{F}_{c_7} = \{u_1, u_2, u_3\}$ have only weak consistency with the observed fault pattern $\mathcal{E}(t) = [-1, -1, 0]^T$ so, they are not considered as potentially faulty to be included in $\mathcal{D}_s$, i.e. $\mathcal{F}_{c_5}, \mathcal{F}_{c_7} \notin \mathcal{D}_s$ whilst $\mathcal{F}_{c_5}, \mathcal{F}_{c_7} \in \mathcal{D}_w$.

6. Simulation results

In this section, simulations are given to illustrate the validity and provide intuition of the theoretical findings of this work. The simulations are based on a five-tank water system, as presented in Ferrari et al. (2009), with the addition of several inputs which are used to verify the proposed actuator fault diagnosis scheme. The structure of the five-tank system is shown in Figure 5, in which it can be seen that the five-tank system is considered connected and decomposed into two distinct and interconnected subsystems. The first three tanks are considered as the first subsystem and the remaining two tanks are considered as the second subsystem.

The dynamics of the first subsystem are given by:

$$\Sigma^{(1)}: \begin{cases} \dot{x}_i^{(1)}(t) = g_i^{(1)}(x^{(1)}(t), u^{(1)}(t)) \\ \quad + h_i^{(1)}(x^{(1)}(t), z^{(1)}(t)) + \eta_i^{(1)}(t) \\ y_i^{(1)}(t) = x_i^{(1)}(t) + \xi_{y,i}^{(1)}(t) \end{cases} \quad i = 1, 2, 3, \tag{46}$$

and the dynamics of the second subsystem are given by

$$\Sigma^{(2)}: \begin{cases} \dot{x}_i^{(2)}(t) = g_i^{(2)}(x^{(2)}(t), u^{(2)}(t)) \\ \quad + h_i^{(2)}(x^{(2)}(t), z^{(2)}(t)) + \eta_i^{(2)}(t) \\ y_i^{(2)}(t) = x_i^{(2)}(t) + \xi_{y,i}^{(2)}(t) \end{cases} \quad i = 1, 2, \tag{47}$$

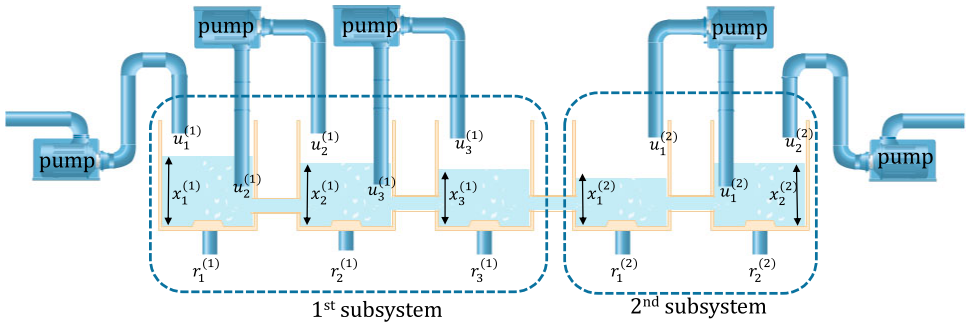

Figure 5. Structure of the considered five-tanks system in this paper.

where $\eta^{(1)} = [\eta_1^{(1)}, \eta_2^{(1)}, \eta_3^{(1)}]^T$ and $\eta^{(2)} = [\eta_1^{(2)}, \eta_2^{(2)}]^T$ denote the modelling uncertainty functions of the first and the second subsystem respectively. The local function dynamics and the interconnection function for subsystem $I = 1$ are:

$$g_1^{(1)}\left(x^{(1)}, u^{(1)}\right) \triangleq 1/S_t\left(u_1^{(1)} - u_2^{(1)} - r_1^{(1)} - \psi(x_2^{(1)}, x_1^{(1)})\right),$$

$$g_2^{(1)}\left(x^{(1)}, u^{(1)}\right) \triangleq 1/S_t\left(u_2^{(1)} - u_3^{(1)} - r_2^{(1)} + \psi(x_2^{(1)}, x_1^{(1)}) - \psi(x_3^{(1)}, x_2^{(1)})\right),$$

$$g_3^{(1)}\left(x^{(1)}, u^{(1)}\right) \triangleq 1/S_t\left(u_3^{(1)} - r_3^{(1)} + \psi(x_3^{(1)}, x_2^{(1)})\right),$$

$$h_3^{(1)}\left(x^{(1)}, z^{(1)}\right) \triangleq 1/S_t\left(-\psi(z^{(1)}, x_3^{(1)})\right),$$

and for subsystem $I = 2$:

$$g_1^{(2)}\left(x^{(2)}, u^{(2)}\right) \triangleq 1/S_t\left(u_1^{(2)} - r_1^{(2)} - \psi(x_2^{(2)}, x_1^{(2)})\right),$$

$$g_2^{(2)}\left(x^{(2)}, u^{(2)}\right) \triangleq 1/S_t\left(u_2^{(2)} - u_1^{(2)} - r_2^{(2)} + \psi(x_2^{(2)}, x_1^{(2)})\right),$$

$$h_1^{(2)}\left(x^{(2)}, z^{(2)}\right) \triangleq 1/S_t\,\psi(x_1^{(2)}, z^{(2)}),$$

where $\psi(v, w) = cs_p\ \mathrm{sign}(w - v)\sqrt{2g|w - v|}$ and the interconnection variable in the first subsystem is $z^{(1)} = x_1^{(2)}$ and in the second subsystem is $z^{(2)} = x_3^{(1)}$. The output flow function $r_i^{(I)}$ of the ith tank of the Ith subsystem is given by

$$r_i^{(I)}(t) = \begin{cases} cs_{r,i}^{(I)}\sqrt{2g\,x_i^{(I)}(t)} & y_i^{(I)}(t) > l_{r,i}^{(I)} \\ 0 & y_i^{(I)}(t) < l_{r,i}^{(I)}, \end{cases} \tag{48}$$

where $l_{r,i}^{(I)}$ is the minimum level of the tank water that keeps the outlet valve of the tank open.

The values used for the simulations are: the gravity constant $g = 9.81\,m/s^2$, the cross section of each tank $S_t = 0.015\,m^2$, the outflow coefficient $c = 1$, the cross section of the connecting pipes $s_p = 5 \times 10^{-4}\,m^2$, the minimum level of the tank water $l_{r,i}^{(I)} = 0.07\,m$ and also, the cross section of the output flow pipes $s_{r,i}^{(I)} = 2 \times 10^{-5}\,m^2$, $I = 1, 2$, $i = 1, \ldots, n_I$.

The nominal functions $g_i^{(1)}$, $i = 1, 2, 3$, and $g_i^{(2)}$, $i = 1, 2$ satisfy the Lipschitz condition with Lipschitz constants $L_{g_i^{(1)}} = \frac{cs_p\sqrt{2g}}{S_t} = 0.1476$, $i = 1, 2, 3$ and also $L_{g_i^{(2)}} = \frac{cs_p\sqrt{2g}}{S_t} = 0.1476$, $i = 1, 2$. The interconnection functions $h_i^{(1)}$, $i = 1, 2, 3$, and $h_i^{(2)}$, $i = 1, 2$ satisfy the Lipschitz condition and hence Lemma 2.1 with known constants $L_{h_3^{(1)}} = \frac{cs_p\sqrt{2g}}{S_t} = 0.1476$ and $L_{h_1^{(2)}} = \frac{cs_p\sqrt{2g}}{S_t} = 0.1476$.

Furthermore, the modelling uncertainty functions are considered as $\eta_1^{(1)}(t) = 0.007\sin(0.7t)$, $\eta_2^{(1)}(t) = 0.006\sin(0.6t)$, $\eta_3^{(1)}(t) = 0.005\cos(0.8t)$, $\eta_1^{(2)}(t) = 0.004\sin(2t)$, and $\eta_2^{(2)}(t) = 0.003\sin(t)$. Thus, the bounding functions are selected as the constants $\bar{\eta}_1^{(1)} = 0.007$, $\bar{\eta}_2^{(1)} = 0.006$, $\bar{\eta}_3^{(1)} = 0.005$, $\bar{\eta}_1^{(2)} = 0.004$, and $\bar{\eta}_2^{(2)} = 0.003$ and hence, the Lipschitz coefficient in (5) is obtained as $L_{\bar{\eta}_i^{(1)}} = 0$, $i = 1, 2, 3$, and $L_{\bar{\eta}_i^{(2)}} = 0$, $i = 1, 2$. Therefore, the coefficient $L_i^{(I)} = L_{h_i^{(I)}} + L_{g_i^{(I)}} + L_{\bar{\eta}_i^{(I)}}$ can be selected as $L_1^{(1)} = 0.2076$, $L_2^{(1)} = 0.1976$, $L_3^{(1)} = 0.3053$, $L_1^{(2)} = 0.3353$, and $L_2^{(2)} = 0.1776$.

The inputs $u_H^{(I)}$ are selected as

$$u_{H,1}^{(1)} = \begin{cases} 0.004\,m^3/s & \text{If } y_1^{(1)} < L_{x_1^{(1)}} \\ 0 & \text{Otherwise,} \end{cases} \tag{49}$$

$$u_{H,2}^{(1)} = \begin{cases} 0.0025\,m^3/s & \text{If } y_1^{(1)} > l_{x_1^{(1)}} \text{ and } y_2^{(1)} < L_{x_2^{(1)}} \\ 0 & \text{Otherwise,} \end{cases} \tag{50}$$

$$u_{H,3}^{(1)} = \begin{cases} 0.0013\,m^3/s & \text{If } y_2^{(1)} > L_{x_2^{(1)}} \text{ and } y_3^{(1)} < L_{x_3^{(1)}} \\ 0 & \text{Otherwise,} \end{cases} \tag{51}$$

for the first subsystem and

$$u_{H,1}^{(2)} = \begin{cases} 0.001\,m^3/s & \text{If } y_1^{(2)} < L_{x_1^{(2)}} \text{ and } y_2^{(2)} > l_{x_2^{(2)}} \\ 0 & \text{Otherwise,} \end{cases} \tag{52}$$

$$u_{H,2}^{(2)} = \begin{cases} 0.002\,m^3/s & \text{If } y_2^{(2)} < L_{x_2^{(2)}} \\ 0 & \text{Otherwise,} \end{cases} \tag{53}$$

for the second subsystem. The constants $l_{x_i^{(I)}}$ and $L_{x_i^{(I)}}$ indicate the minimum and the maximum level of the water in the tank respectively, which is considered as $l_{x_i^{(I)}} = 0.07\,m$ and $L_{x_i^{(I)}} = 2\,m$ for $I = 1$, $i = 1, 2, 3$ and for $I = 2$, $i = 1, 2$. Furthermore, the parameters $\alpha_i^{(I)}$ and $\lambda_i^{(I)}$, that determine the fault pattern function $\beta_i^{(I)}$, for $I = 1$, $i = 1, 2, 3$ and for $I = 2$, $i = 1, 2$, are selected in a way that produce different fault types, i.e. incipient/abrupt and also different rate of actuator loss of effectiveness. Specifically, $\alpha_i^{(I)}$ is selected as $\alpha_i^{(I)} = 0.5$, for all actuators,

to adjust the loss of effectiveness percentage to 50% of their values in healthy condition, and use different values for the fault evolution rate $\lambda_1^{(I)} = 1$, $\lambda_2^{(I)} = 0.1$, $\forall I = 1, 2$ and $\lambda_3^{(1)} = 0.01$. It is worth mentioning that when an input value $u_{H,i}^{(I)}$ is set to zero, then any fault in that actuator is vanished.

As described in Section 3, the matrix $K^{(I)}$ is selected as $K^{(I)} = A^{(I)} + M^{(I)}$ where $M^{(I)} = \text{diag}\{\mu_1^{(I)}, \ldots, \mu_{n_I}^{(I)}\}$, $\mu_i^{(I)} > L_i^{(I)}, 1 = 1, \ldots, n_I$, $I = 1, 2$. To this end, the diagonal matrix $M^{(I)}$ is selected as $M^{(1)} = \text{diag}\{12, 13, 14\}$ and $M^{(2)} = \text{diag}\{5, 7\}$ and, since $A^{(I)} = 0_{n_I \times n_I}$, $I = 1, 2$, therefore, the observer gain matrices $K^{(I)}$, $I = 1, 2$ are obtained as $K^{(1)} = \text{diag}\{12, 13, 14\}$ and $K^{(2)} = \text{diag}\{5, 7\}$.

In the simulations, the sensor noise $\xi_{y,i}^{(I)}$ is considered Gaussian with zero mean and variance $\sigma^2_{\xi_{y_i}^{(I)}} = 1 \times 10^{-6}$, for all $i = 1, \ldots, n_I$, $I = 1, 2$. Therefore, an appropriate bound for the sensor noise $\xi_{y,i}^{(I)}$ with this variance can be selected as $\bar{\xi}_{y,i}^{(I)} = 0.0058$ m, $i = 1, \ldots, n_I$, $I = 1, 2$ which is obtained as the maximum value from 10^{+7} random iterations. Furthermore, since $\xi_z^{(I)} = y_z^{(I)} - z^{(I)}$, the bound $\bar{\xi}_z^{(I)}$ can be determined by considering the value of its corresponding sensor noise thresholds. Therefore, $\bar{\xi}_z^{(1)} = \bar{\xi}_{y,1}^{(2)}$ and also $\bar{\xi}_z^{(2)} = \bar{\xi}_{y,3}^{(1)}$, where $\bar{\xi}_y^{(I)}$ is the threshold value of the sensor noise $\xi_y^{(I)}$.

Since the objective of this paper is to diagnose multiple actuator faults that occur at different actuators and at different times, we consider two different situations: (a) single fault occurrence and, (b) multiple faults occurrence. In the first situation, one case is considered, in which a single abrupt actuator fault occurs at the actuator $u_1^{(1)}$ of subsystem $I = 1$ at time $T_{0,1}^{(1)} = 5$ s, whilst the actuators $u_2^{(1)}$ and $u_3^{(1)}$ of subsystem $I = 1$ and also all the actuators of subsystem $I = 2$ are considered healthy. In the second situation with multiple actuator faults, two cases are considered: (i) only the first subsystem becomes faulty, specifically the actuators $u_1^{(1)}$ and $u_2^{(1)}$ of subsystem $I = 1$ become faulty at times $T_{0,1}^{(1)} = 5$ s and $T_{0,2}^{(1)} = 10$ s, respectively, whilst, the actuator $u_3^{(1)}$ of the subsystem $I = 1$ and all actuators of subsystem $I = 2$ are healthy. and, (ii) both subsystems become faulty and specifically actuators $u_1^{(1)}$, $u_2^{(1)}$ and $u_1^{(2)}$ become faulty at times $T_{0,1}^{(1)} = 5$ s, $T_{0,2}^{(1)} = 10$ s and $T_{0,1}^{(2)} = 8$ s, respectively (in this case, the actuators $u_3^{(1)}$ of the subsystem $I = 1$ and $u_2^{(2)}$ of the subsystem $I = 2$ remain healthy).

The simulation results regarding the first situation with the single actuator fault in actuator $u_1^{(1)}$ of subsystem $I = 1$ is shown in Figure 6. Furthermore, the result from the output $y_1^{(1)}$ and the faulty actuator $u_1^{(1)}$ is given in Figure 7. As it can be seen from Figure 6, in the detection agent of subsystem $I = 1$ (see Figure 6(a)), the residual $y_1^{(1)}$ exceeds (in absolute value) its corresponding threshold $\bar{y}_1^{(1)}$ shortly after the fault occurrence and specifically at time $T_{d,1}^{(1)} = 5.3$ s, and continues to exceed it until the time $t = 35.1$ s. At this time, the level of the water in tank 1, as it can be seen at Figure 7(a), reaches its maximum threshold value ($L_{x_1^{(1)}} = 2\,m$) and the actuator output value $u_1^{(1)}$ begins to oscillate between its faulty value and zero (see Figure 7(b)). As a result, the residual is bounded by the threshold, i.e. $|\tilde{y}_1^{(1)}(t)| < \bar{y}_1^{(1)}(t)$, for $t \in [35.1, 60]$ s. In addition, as it can be seen from Figure 6(b,c), the actuator fault is not detected in the other states of the subsystem $I = 1$, a result that is in line with Remark 2.1. Furthermore, in the detection agent of subsystem $I = 2$ (see Figure 6(d,e)), it can be seen that no fault is detected since the residuals do not exceed their corresponding thresholds, a result that is line with Lemma 4.1. At time $T_{d,1}^{(1)} = 5.3$, when the actuator fault is detected in subsystem $I = 1$, the fault isolation agent of subsystem $I = 1$ is activated.

Considering the sign of the input values of $u_i^{(1)}$, $i = 1, 2, 3$ in Equation (46), which are all positive in this simulation example, the signature matrix defined in (39) is calculated based on the

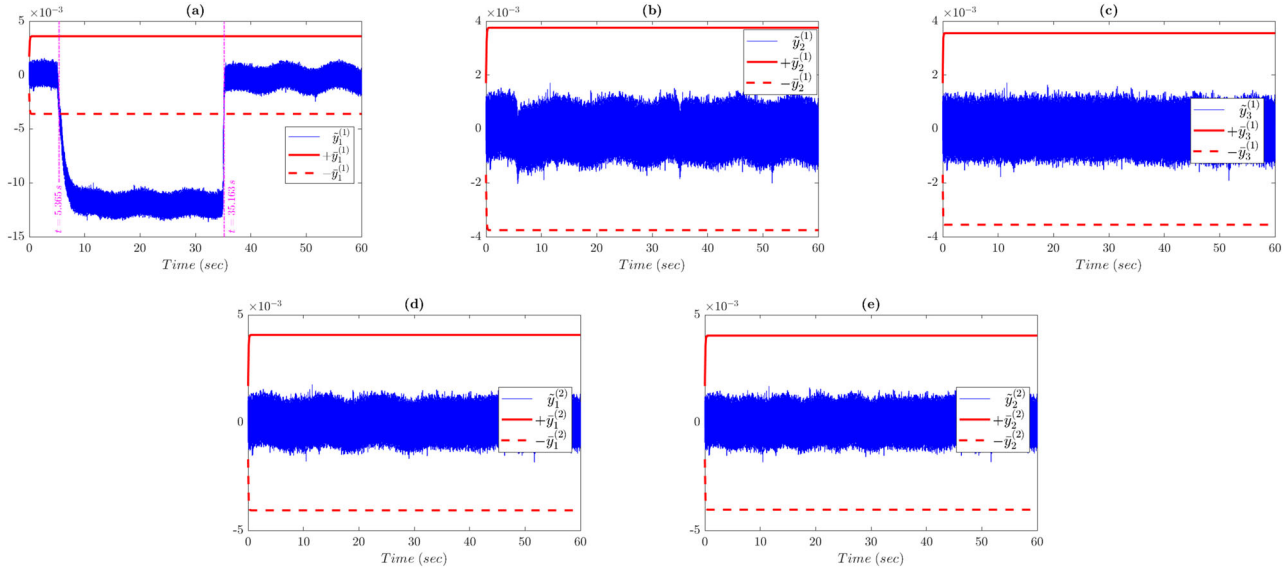

Figure 6. Single actuator fault case of actuator $u_1^{(1)}$ in subsystem $I = 1$ at time $T_{0,1}^{(1)} = 5$ sec. Residuals and corresponding thresholds for the detection agent for subsystem $I = 1$ are shown in subfigures (a), (b) and (c) and for $I = 2$ in (d) and (e).

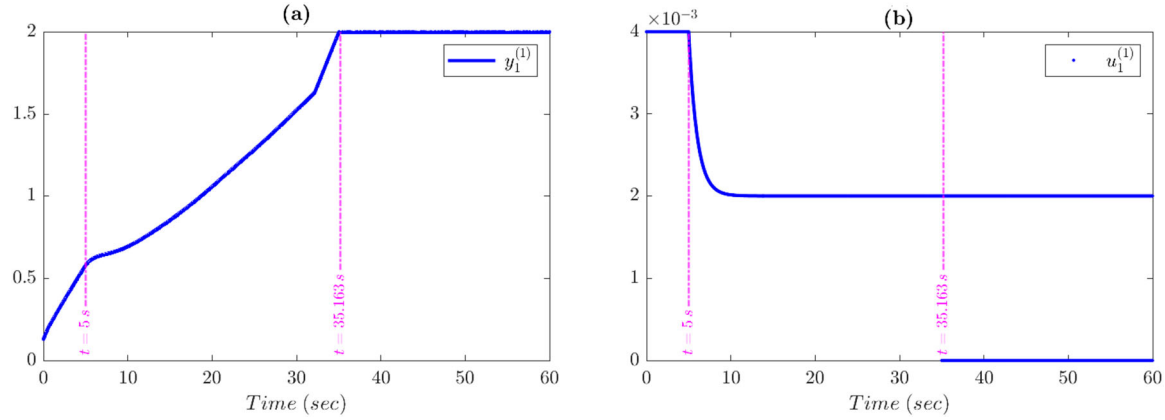

Figure 7. Single actuator fault case of actuator $u_1^{(1)}$ in subsystem $I = 1$ at time $T_{0,1}^{(1)} = 5$ sec. The residual $\tilde{y}_1^{(1)}$ and its corresponding thresholds are given in Figure 6(a). The behaviour of output $y_1^{(1)}$ is presented in subfigure (a), and the behaviour of the faulty actuator $u_1^{(1)}$ is given in subfigure (b).

reasoning explained after (39) as follows:

$$F^{(1)} = \begin{array}{c} \begin{matrix} \mathcal{F}_{c_1}^{(1)} & \mathcal{F}_{c_2}^{(1)} & \mathcal{F}_{c_3}^{(1)} & \mathcal{F}_{c_4}^{(1)} & \mathcal{F}_{c_5}^{(1)} & \mathcal{F}_{c_6}^{(1)} & \mathcal{F}_{c_7}^{(1)} \end{matrix} \\ \begin{pmatrix} -1 & +1 & 0 & * & -1 & +1 & * \\ 0 & -1 & +1 & -1 & +1 & * & * \\ 0 & 0 & -1 & 0 & -1 & -1 & -1 \end{pmatrix} \end{array} \tag{54}$$

where each column of this matrix corresponds to each of the following fault combination sets: $\mathcal{F}_{c_1}^{(1)} = \{u_1^{(1)}\}$, $\mathcal{F}_{c_2}^{(1)} = \{u_2^{(1)}\}$, $\mathcal{F}_{c_3}^{(1)} = \{u_3^{(1)}\}$, $\mathcal{F}_{c_4}^{(1)} = \{u_1^{(1)}, u_2^{(1)}\}$, $\mathcal{F}_{c_5}^{(1)} = \{u_1^{(1)}, u_3^{(1)}\}$, $\mathcal{F}_{c_6}^{(1)} = \{u_2^{(1)}, u_3^{(1)}\}$, and $\mathcal{F}_{c_7}^{(1)} = \{u_1^{(1)}, u_2^{(1)}, u_3^{(1)}\}$.The signature matrix of the second subsystem $F^{(2)}$ is calculated as follows:

$$F^{(2)} = \begin{array}{c} \begin{matrix} \mathcal{F}_{c_1}^{(2)} & \mathcal{F}_{c_2}^{(2)} & \mathcal{F}_{c_3}^{(2)} \end{matrix} \\ \begin{pmatrix} -1 & 0 & -1 \\ +1 & +1 & * \end{pmatrix} \end{array} \tag{55}$$

where each column of this matrix corresponds to each of the following fault combination sets: $\mathcal{F}_{c_1}^{(2)} = \{u_1^{(2)}\}$, $\mathcal{F}_{c_2}^{(2)} = \{u_2^{(2)}\}$ and $\mathcal{F}_{c_3}^{(2)} = \{u_1^{(2)}, u_2^{(2)}\}$. Note that, since the signs of the actuators' outputs never change (always positive), therefore the signature matrices are always given by (54) and (55).

Considering the observed pattern of the actuator fault vector $\mathcal{E}^{(1)}(t) = [-1\,0\,0]^T$ during the interval $[T_{d,1}^{(1)} = 5.3, 35.1]$ sec (see Figure 6(a–c)) and, by applying the isolation Algorithm 1, the diagnosis set $\mathcal{D}_s^{(1)}(t)$ of the faulty actuator sets is obtained as:

$$\mathcal{D}_s^{(1)} = \left\{\mathcal{F}_{c_1}^{(1)}\right\} = \left\{\{u_1^{(1)}\}\right\}, \tag{56}$$

which shows that the potential diagnosis set defined in our proposed approach can precisely isolate the faulty actuator. The diagnosed pattern of actuator fault sets obtained via weak consistency is

$$\begin{aligned} \mathcal{D}_w^{(1)} &= \left\{\mathcal{F}_{c_1}^{(1)}, \mathcal{F}_{c_4}^{(1)}, \mathcal{F}_{c_5}^{(1)}, \mathcal{F}_{c_7}^{(1)}\right\} \\ &= \left\{\{u_1^{(1)}\}, \{u_1^{(1)}, u_2^{(1)}\}, \{u_1^{(1)}, u_3^{(1)}\}, \{u_1^{(1)}, u_2^{(1)}, u_3^{(1)}\}\right\}, \end{aligned} \tag{57}$$

which includes the faulty actuator but, as mentioned earlier $\mathcal{D}_w^{(I)}$ contains always the actual faulty actuator set with the downside that is contains many suspected fault sets. However, as mentioned earlier the intersection set $\mathcal{F}_w^{(1)}(t)$, gives the actuators that are definitely faulty which in this case is $\mathcal{F}_w^{(1)}(t) = \{u_1^{(1)}\}$. In general, the overall obtained simulation results for this case are given in Table 2.

The simulation results for the case b(i) (multiple actuator fault occurrences in only subsystem $I = 1$, $u_1^{(1)}, u_2^{(1)}$ become faulty) are shown in Figure 8. As it can be seen from this figure, both faults were detected. Specifically, the residual $\tilde{y}_1^{(1)}$ exceeds its corresponding threshold at time $T_{d,1}^{(1)} = 5.3$ sec, which according to Remark 4.1 means that actuators $u_1^{(1)}$ and/or $u_2^{(1)}$ is/are faulty. In addition, the residual $\tilde{y}_2^{(1)}$ exceeds its corresponding threshold at time $T_{d,2}^{(1)} = 15.6$ sec which according

Table 2. The obtained simulation results for the single actuator fault case depicted in Figure 6.

Time interval	$[0, T_0^{(1)}) =$ [0, 5) sec	$[T_0^{(1)}, T_{d,1}^{(1)}) =$ [5, 5.3) sec	$[T_{d,1}^{(1)}, 35.1) =$ [5.3, 35.1) sec	[35.1, 60] sec
Actual faulty actuators	–	$\mathcal{F}_{\mathbf{c_1}}^{(\mathbf{1})} = \{\mathbf{u_1^{(1)}}\}$	$\mathcal{F}_{\mathbf{c_1}}^{(\mathbf{1})} = \{\mathbf{u_1^{(1)}}\}$	–
Observed pattern $\mathcal{E}^{(1)}(t)$		$[0, 0, 0]^T$	$[-1, 0, 0]^T$	$[0, 0, 0]^T$
Diagnosis sets $\mathcal{D}_s^{(1)}(t)$ (consistency)		–	$\{\mathcal{F}_{c_1}^{(1)}\}$	–
Diagnosis sets $\mathcal{D}_w^{(1)}(t)$ (weak consistency)		–	$\{\mathcal{F}_{c_1}^{(1)}, \mathcal{F}_{c_4}^{(1)}, \mathcal{F}_{c_5}^{(1)}, \mathcal{F}_{c_7}^{(1)}\}$	–
Faulty identified set $\mathcal{F}_w^{(1)}(t)$		–	$\mathcal{F}_{\mathbf{c_1}}^{(\mathbf{1})} = \{\mathbf{u_1^{(1)}}\}$	–

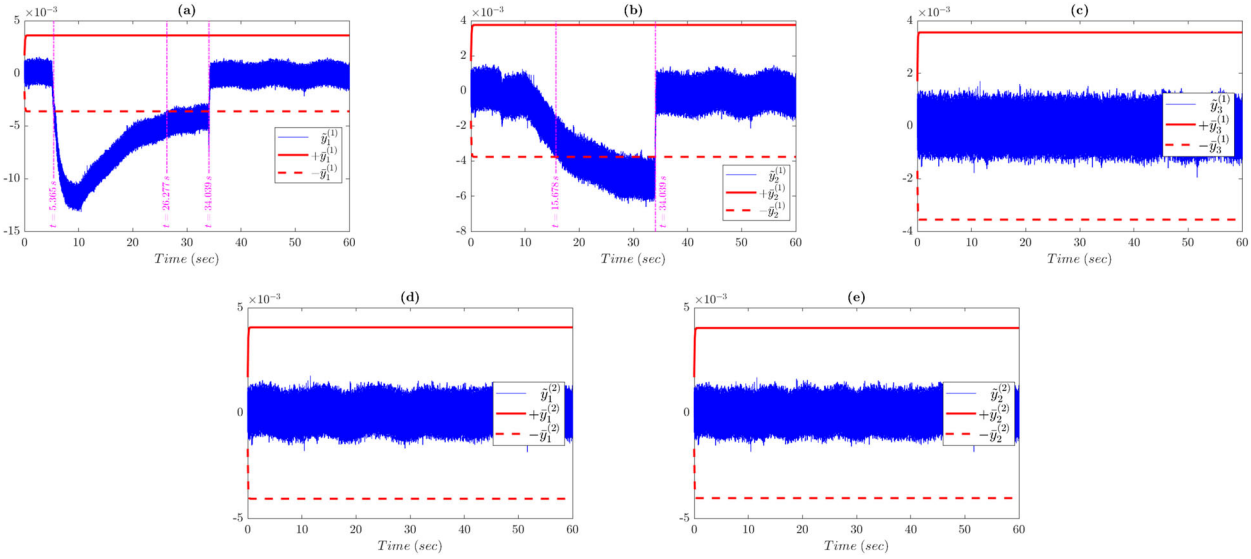

Figure 8. Multiple actuator faults case, where faults in actuators $u_1^{(1)}$ and $u_2^{(1)}$ of subsystem $I = 1$ occur at time $T_{0,1}^{(1)} = 5$ sec and at time $T_{0,2}^{(1)} = 10$ sec, respectively. Residuals and corresponding thresholds for the detection agent for subsystem $I = 1$ are shown in subfigures (a), (b) and (c) and for $I = 2$ in (d) and (e).

to Remark 4.1 means that actuators $u_2^{(1)}$ and/or $u_3^{(1)}$ is/are also faulty.

At time $T_{d,1}^{(1)} = 5.3$ sec, the fault is detected in the residual $\tilde{y}_1^{(1)}$, i.e. $\mathcal{E}^{(1)} = [-1\,0\,0]^T$, and hence, the fault isolation agent of the first subsystem is activated. From $T_{d,1}^{(1)} = 5.3$ sec (when the fault in actuator $u_1^{(1)}$ causes the residual $\tilde{y}_1^{(1)}$ to exceed its corresponding threshold $\bar{y}_1^{(1)}$) and until the second fault occurs (at $t = 10$ sec) and gets detected at time $t = T_{d,2}^{(1)} = 15.6$ sec, the observed pattern of the actuator fault vector $\mathcal{E}^{(1)}(t) = [-1\,0\,0]^T$. As a result, the diagnosis set remains the same as the previous case, i.e. $\mathcal{D}_s^{(1)} = \{\mathcal{F}_{c_1}^{(1)}\} = \{\{u_1^{(1)}\}\}$, and $\mathcal{D}_w^{(1)} = \{\mathcal{F}_{c_1}^{(1)}, \mathcal{F}_{c_4}^{(1)}, \mathcal{F}_{c_5}^{(1)}, \mathcal{F}_{c_7}^{(1)}\}$. As a result, the intersection set $\mathcal{F}_w^{(1)}(t) = \{u_1^{(1)}\}$, which indicates that $u_1^{(1)}$ is correctly identified as a faulty actuator. During the time interval $[T_{d,2}^{(1)}, 34.0]$ sec, the residual $\tilde{y}_2^{(1)}$ also exceeds its corresponding threshold $\bar{y}_2^{(1)}$, i.e. $\tilde{y}_2^{(1)} < -\bar{y}_2^{(1)}$. The faults in $u_1^{(1)}$ and $u_2^{(1)}$ are both detected during the time interval $[T_{d,2}^{(1)}, 26.2]$ sec and, the observed pattern of the actuator fault in the subsystem $I = 1$ during this interval becomes $\mathcal{E}^{(1)}(t) = [-1\ -1\,0]^T$ (see Figures 8(a–c)). Then according to the isolation Algorithm 1, the diagnosis fault sets for this time interval are obtained as

$$\mathcal{D}_s^{(1)}(t) = \left\{\mathcal{F}_{c_4}^{(1)}\right\} = \left\{\{u_1^{(1)}, u_2^{(1)}\}\right\}, \tag{58}$$

indicating that the faulty actuators are $\{u_1^{(1)}, u_2^{(1)}\}$, which is the correct set. Furthermore, the diagnosed pattern of actuator fault sets obtained via weak consistency for the same time interval is

$$\mathcal{D}_w^{(1)}(t) = \left\{\mathcal{F}_{c_4}^{(1)}, \mathcal{F}_{c_7}^{(1)}\right\} = \left\{\{u_1^{(1)}, u_2^{(1)}\}, \{u_1^{(1)}, u_2^{(1)}, u_3^{(1)}\}\right\}, \tag{59}$$

and as a result, the intersection set $\mathcal{F}_w^{(1)}(t) = \{u_1^{(1)}, u_2^{(1)}\}$, which declares that $u_1^{(1)}$ and $u_2^{(1)}$ are correctly identified as faulty actuators.

Meanwhile there are some times in the interval $t \in [26.2, 34.0]$ sec where both faults in actuators $u_1^{(1)}$ and $u_2^{(1)}$ neutralise each other's effects. As a result, the subsystem $I = 1$ does not show any fault, i.e. $|\tilde{y}_1^{(1)}| < \bar{y}_1^{(1)}$ for some times in $t \in [26.2, 34.0]$ sec. Thus, the observed pattern of the actuator fault in subsystem $I = 1$ is $\mathcal{E}^{(1)} = [0\ -1\,0]^T$. Then, by applying the isolation Algorithm 1, the diagnosis fault sets $\mathcal{D}_s^{(1)}$ are found to be empty. The weak consistency condition gives $\mathcal{D}_w^{(1)} = \{\mathcal{F}_{c_2}^{(1)}, \mathcal{F}_{c_4}^{(1)}, \mathcal{F}_{c_6}^{(1)}, \mathcal{F}_{c_7}^{(1)}\} = \{\{u_2^{(1)}\}, \{u_1^{(1)}, u_2^{(1)}\}, \{u_2^{(1)}, u_3^{(1)}\}, \{u_1^{(1)}, u_2^{(1)}, u_3^{(1)}\}\}$ and as a result, the intersection set $\mathcal{F}_w^{(1)}(t) = \{u_2^{(1)}\}$, which declares that $u_2^{(1)}$ is correctly identified as a faulty actuator.

Finally, at time $t = 34.0$ sec, the water level in both tanks related to the outputs $y_1^{(1)}$ and $y_2^{(1)}$ reach their corresponding threshold values $L_{x_1^{(1)}}$ and $L_{x_2^{(1)}}$, respectively defined in (49) and (50). Then, the actuators $u_1^{(1)}$ and $u_2^{(1)}$ are set to zero since the flow stops. As a result the actuator faults cannot be observed, i.e. $\mathcal{E}^{(1)}(t) = [0\,0\,0]^T$ for all $t \in [34.0, 60]$. In general, the overall obtained simulation results for this case are given in Table 3.

Finally, the simulation is done for the case b(ii) (multiple actuator fault occurrences in both subsystems $I = 1, 2$) and the results are shown in Figure 9. As can be seen, all faults which occurred at time $T_{0,1}^{(1)} = 5$ sec, $T_{0,2}^{(1)} = 10$ sec, and $T_{0,1}^{(2)} = 8$ sec are detected by their respective detection agents, shortly after and specifically at times $T_{d,1}^{(1)} = 5.3$ sec, $T_{d,2}^{(1)} = 15.6$ sec, for the first and the second state of the subsystem $I = 1$, respectively; and at time $T_{d,1}^{(2)} = 13.9$ sec and $T_{d,2}^{(2)} = 14.1$ sec for the first and the second state of subsystem $I = 2$, respectively.

The actuator fault isolation results in subsystem $I = 1$ is exactly the same as in the previous case (b)(i) that was discussed earlier and hence, the diagnosis fault sets are given in Table 3.

The fault in subsystem $I = 2$ is detected at time $t = T_{d,1}^{(2)} = 13.9$ sec (see Figure 9(d)) and at that point the corresponding fault isolation module is activated. As can be seen in Figure 9(d,e), there are some time instances that the observed

Table 3. The obtained simulation results for the single actuator fault case depicted in Figure 8.

Time interval	$[0, T_{0,1}^{(1)})=$ [0, 5) sec	$[T_{0,1}^{(1)}, T_{d,1}^{(1)})=$ [5, 5.3) sec	$[T_{d,1}^{(1)}, T_{0,2}^{(1)})=$ [5.3, 10) sec	$[T_{0,2}^{(1)}, T_{d,2}^{(1)})=$ [10, 15.6) sec	$[T_{d,2}^{(1)}, 26.2)=$ [15.6, 26.2) sec	[26.2, 34.0) sec
Actual faulty actuators	–	$\mathcal{F}_{\mathbf{c_1}}^{(\mathbf{1})} = \{\mathbf{u_1}^{(\mathbf{1})}\}$	$\mathcal{F}_{\mathbf{c_1}}^{(\mathbf{1})} = \{\mathbf{u_1}^{(\mathbf{1})}\}$	$\mathcal{F}_{\mathbf{c_4}}^{(\mathbf{1})} = \{\mathbf{u_1}^{(\mathbf{1})}, \mathbf{u_2}^{(\mathbf{1})}\}$	$\mathcal{F}_{\mathbf{c_4}}^{(\mathbf{1})} = \{\mathbf{u_1}^{(\mathbf{1})}, \mathbf{u_2}^{(\mathbf{1})}\}$	$\mathcal{F}_{\mathbf{c_4}}^{(\mathbf{1})} = \{\mathbf{u_1}^{(\mathbf{1})}, \mathbf{u_2}^{(\mathbf{1})}\}$
Observed pattern $\mathcal{E}^{(1)}(t)$		$[0, 0, 0]^T$		$[-1, 0, 0]^T$	$[-1, -1, 0]^T$	$[0, -1, 0]^T$
Diagnosis sets $\mathcal{D}_s^{(1)}(t)$ (consistency)		–		$\{\mathcal{F}_{c_1}^{(1)}\}$	$\{\mathcal{F}_{c_4}^{(1)}\}$	{}
Diagnosis sets $\mathcal{D}_w^{(1)}(t)$ (weak consistency)		–	$\{\mathcal{F}_{c_1}^{(1)}, \mathcal{F}_{c_4}^{(1)}, \mathcal{F}_{c_5}^{(1)}, \mathcal{F}_{c_7}^{(1)}\}$		$\{\mathcal{F}_{c_4}^{(1)}, \mathcal{F}_{c_7}^{(1)}\}$	$\{\mathcal{F}_{c_2}^{(1)}, \mathcal{F}_{c_4}^{(1)}, \mathcal{F}_{c_6}^{(1)}, \mathcal{F}_{c_7}^{(1)}\}$
Faulty identified set $\mathcal{F}_w^{(1)}(t)$		–	$\mathcal{F}_{\mathbf{c_1}}^{(\mathbf{1})} = \{\mathbf{u_1}^{(\mathbf{1})}\}$		$\mathcal{F}_{\mathbf{c_4}}^{(\mathbf{1})} = \{\mathbf{u_1}^{(\mathbf{1})}, \mathbf{u_2}^{(\mathbf{1})}\}$	$\mathcal{F}_{\mathbf{c_2}}^{(\mathbf{1})} = \{\mathbf{u_2}^{(\mathbf{1})}\}$

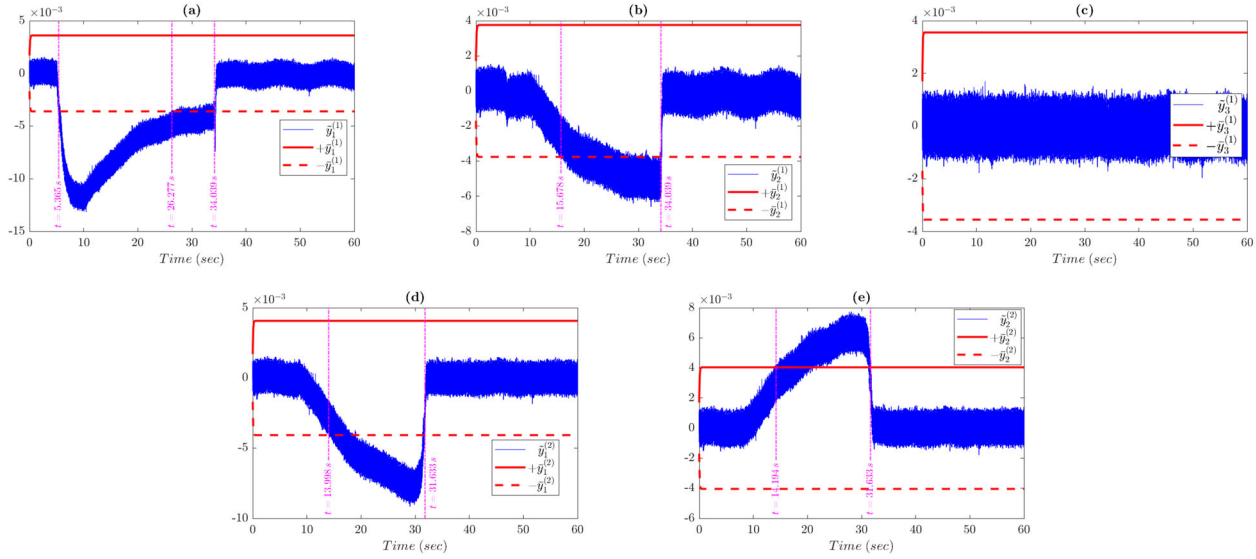

Figure 9. Multiple actuator fault case, where the faults in $l = 1$ occur in actuators $u_1^{(1)}$ and $u_2^{(1)}$ at times $T_{0,1}^{(1)} = 5$ sec and $T_{0,2}^{(1)} = 10$ sec, respectively, and for $l = 2$ the fault occurs in $u_1^{(2)}$ at time $T_{0,1}^{(2)} = 8$ sec. Residuals and corresponding thresholds for the detection agent for subsystem $l = 1$ are shown in subfigures (a), (b) and (c) and for $l = 2$ in (d) and (e).

pattern of the actuator faults can only be detected by the violation of the residual $\tilde{y}_1^{(2)}$, i.e. for all $t \in [T_{d,1}^{(2)}, T_{d,2}^{(2)}] = [13.9, 14.1]$ sec. In this case, the observed pattern of actuator fault is $\mathcal{E}^{(2)} = [-1\ 0]^T$ and, by applying the Algorithm 1, the diagnosis fault set for the second subsystem is obtained as $\mathcal{D}_s^{(2)} = \{\}$, whereas by using the weak consistency condition, the diagnosis fault set $\mathcal{D}_w^{(2)}$ is obtained as:

$$\mathcal{D}_w^{(2)} = \left\{\mathcal{F}_{c_1}^{(2)}, \mathcal{F}_{c_3}^{(2)}\right\} = \left\{\{u_1^{(2)}\}, \{u_1^{(2)}, u_2^{(2)}\}\right\}, \qquad (60)$$

as a result, $\mathcal{F}_w^{(2)}(t) = \{u_1^{(2)}\}$, which declares that $u_1^{(2)}$ is correctly identified as a faulty actuator.

During the time $t \in [T_{d,2}^{(2)} = 14.1, 31.6]$ sec, where the fault is detected in both residuals $\tilde{y}_1^{(2)}$ and $\tilde{y}_2^{(2)}$, the observed pattern of the actuator fault vector is $\mathcal{E}^{(2)}(t) = [-1\ +1]^T$ and the Algorithm 1 results in the same diagnosis fault sets for $I = 2$ by using the consistency and weak consistency condition, i.e.:

$$\mathcal{D}_s^{(2)}(t) = \mathcal{D}_w^{(2)}(t) = \left\{\mathcal{F}_{c_1}^{(2)}, \mathcal{F}_{c_3}^{(2)}\right\} = \left\{\{u_1^{(2)}\}, \{u_1^{(2)}, u_2^{(2)}\}\right\}, \qquad (61)$$

as a result, the intersection set $\mathcal{F}_w^{(2)}(t) = \{u_1^{(2)}\}$, which declares that $u_1^{(2)}$ is correctly identified as a faulty actuator.

Table 4. The obtained simulation results for the multiple actuator fault cases depicted in Figure 9.

Time interval	$[0, T_{0,1}^{(2)})=$ [0, 8) sec	$[T_{0,1}^{(2)}, T_{d,1}^{(2)})=$ [8, 13.9) sec	$[T_{d,1}^{(2)}, T_{d,2}^{(2)})=$ [13.9, 14.1) sec	$[T_{d,2}^{(2)}, 31.6)=$ [14.1, 31.6) sec	[31.6, 60] sec
Actual faulty actuators	–	$\mathcal{F}_{\mathbf{c_1}}^{(\mathbf{2})} = \{\mathbf{u_1}^{(\mathbf{2})}\}$	$\mathcal{F}_{\mathbf{c_1}}^{(\mathbf{2})} = \{\mathbf{u_1}^{(\mathbf{2})}\}$	$\mathcal{F}_{\mathbf{c_1}}^{(\mathbf{2})} = \{\mathbf{u_1}^{(\mathbf{2})}\}$	–
Observed pattern $\mathcal{E}^{(2)}(t)$		$[0, 0]^T$	$[-1, 0]^T$	$[-1, +1]^T$	$[0, 0]^T$
Diagnosis sets $\mathcal{D}_s^{(2)}(t)$ (consistency)		–	{}	$\{\mathcal{F}_{c_1}^{(2)}, \mathcal{F}_{c_3}^{(2)}\}$	–
Diagnosis sets $\mathcal{D}_w^{(2)}(t)$ (weak consistency)		–	$\{\mathcal{F}_{c_1}^{(2)}, \mathcal{F}_{c_3}^{(2)}\}$	$\{\mathcal{F}_{c_1}^{(2)}, \mathcal{F}_{c_3}^{(2)}\}$	–
Faulty identified set $\mathcal{F}_w^{(2)}(t)$		–	$\mathcal{F}_{\mathbf{c_1}}^{(\mathbf{2})} = \{\mathbf{u_1}^{(\mathbf{2})}\}$	$\mathcal{F}_{\mathbf{c_1}}^{(\mathbf{2})} = \{\mathbf{u_1}^{(\mathbf{2})}\}$	–

After the time $t > 31.6$, where the level of water in the corresponding tank of actuator $u_1^{(2)}$ reaches its maximum value (and as a result actuator $u_1^{(2)}$ is set to zero), the fault is not detected in both residuals $\tilde{y}_1^{(2)}$ and $\tilde{y}_2^{(2)}$, i.e. the observed pattern of actuator fault is $\mathcal{E}^{(2)}(t) = [0\,0]^T,\ \forall\, t \in [31.6, 60]$. The overall obtained simulation results for this case (b(ii)) are given in Table 4.

7. Conclusion

This paper deals with the problem of actuator fault detection and isolation in a class of nonlinear interconnected systems. The fault detection scheme is conducted on a distributed framework mimicking the structure of the interconnected subsystems and, it is comprised of having a detection agent monitoring each subsystem for possible actuator faults. Suitable detection thresholds that guarantee no false alarms are designed. In addition, the fault propagation issue is investigated and, as it is shown an actuator fault occurring in one subsystem can only be detected by its corresponding detection agent, hence leading to the identification of the faulty subsystem. Multiple actuator fault isolation is investigated via designing a reasoning-based decision logic process which benefits from the concepts of signature matrix and inverse set-enumeration tree allowing to identify the potential faulty actuator sets. Future work will focus on the diagnosis of multiple actuators and sensors in large-scale interconnected nonlinear dynamical systems.

Disclosure statement

No potential conflict of interest was reported by the author(s).

Funding

This work has been supported by the European Union's Horizon 2020 research and innovation programme under grant agreement No 739551 (KIOS CoE), the Government of the Republic of Cyprus through the Directorate General for European Programmes, Coordination and Development, and European Research Council (ERC) under the ERC Synergy Grant Water-Futures (Grant agreement No. 951424).

References

Arrichiello, F., Marino, A., & Pierri, F. (2015). Observer-based decentralized fault detection and isolation strategy for networked multirobot systems. *IEEE Transactions on Control Systems Technology*, *23*(4), 1465–1476. https://doi.org/10.1109/TCST.2014.2377175

Bartys, M. (2015a). Diagnosing multiple faults from FDI perspective. In Z., Kowalczuk & M., Domżalski. *Advanced Systems for Automation and Diagnostics*. Pomorskie Wydawnictwo Naukowo-Techniczne, ISBN 978-83-63177-00-3.

Bartys, M. (2015b). Diagnosing multiple faults with the dynamic binary matrix. In *9th IFAC Symposium on Fault Detection, Supervision and Safety for Technical Processes* (vol. 48, no. 21, pp. 1297–1302). IFAC-PapersOnLinef.

Blanke, M., Kinnaert, M., Lunze, J., Staroswiecki, M., & Schröder, J. (2006). *Diagnosis and fault-tolerant control*. Springer. *2*, 1–32.

Boem, F., Ferrari, R. M., Keliris, C., Parisini, T., & Polycarpou, M. M. (2016). A distributed networked approach for fault detection of large-scale systems. *IEEE Transactions on Automatic Control*, *62*(1), 18–33. https://doi.org/10.1109/TAC.2016.2539326

Boem, F., Ferrari, R. M., & Parisini, T. (2011). Distributed fault detection and isolation of continuous-time non-linear systems. *European Journal of Control*, *17*(5-6), 603–620. https://doi.org/10.3166/ejc.17.603-620

Boem, F., Ferrari, R. M., Parisini, T., & Polycarpou, M. M. (2013). Distributed fault diagnosis for continuous-time nonlinear systems: The input–output case. *Annual Reviews in Control*, *37*(1), 163–169. https://doi.org/10.1016/j.arcontrol.2013.03.008

Caccavale, F., Pierri, F., & Villani, L. (2008). Adaptive observer for fault diagnosis in nonlinear discrete-time systems. *ASME Journal of Dynamic Systems, Measurement, and Control*, *130*(2), 021005 (9 pages). https://doi.org/10.1115/1.2837310

Chen, J., & Patton, R. J. (2012). *Robust model-based fault diagnosis for dynamic systems* (Vol. 3). Springer Science & Business Media.

Chen, T., Zhu, Z., Wang, C., & Dong, Z. (2021). Rapid sensor fault diagnosis for a class of nonlinear systems via deterministic learning. *IEEE Transactions on Neural Networks and Learning Systems*, *33*(12), 7743–7754. https://doi.org/10.1109/TNNLS.2021.3087533

Chen, W., Chen, W. T., Saif, M., Li, M. F., & Wu, H. (2013). Simultaneous fault isolation and estimation of lithium-ion batteries via synthesized design of Luenberger and learning observers. *IEEE Transactions on Control Systems Technology*, *22*(1), 290–298. https://doi.org/10.1109/TCST.2013.2239296

Cordier, M. O., Dague, P., Lévy, F., Montmain, J., Staroswiecki, M., & Travé-Massuyès, L. (2004). Conflicts versus analytical redundancy relations: A comparative analysis of the model based diagnosis approach from the artificial intelligence and automatic control perspectives. *IEEE Transactions on Systems, Man, and Cybernetics, Part B (Cybernetics)*, *34*(5), 2163–2177. https://doi.org/10.1109/TSMCB.2004.835010

Davoodi, M. R., Khorasani, K., Talebi, H. A., & Momeni, H. R. (2013). Distributed fault detection and isolation filter design for a network of heterogeneous multiagent systems. *IEEE Transactions on Control Systems Technology*, *22*(3), 1061–1069. https://doi.org/10.1109/TCST.87

De Kleer, J., & Kurien, J. (2003). Fundamentals of model-based diagnosis. In *Proceedings 5th IFAC Symp', Fault Detection, Supervision, Safety Technical Processes (SAFEPROCESS)* (vol. 36, no. 5, pp. 25–36). IFAC Proceedings.

Ding, S. X. (2008). *Model-based fault diagnosis techniques: Design schemes, algorithms, and tools*. Springer Science & Business Media.

Du, M., & Mhaskar, P. (2014). Isolation and handling of sensor faults in nonlinear systems. *Automatica*, *50*(4), 1066–1074. https://doi.org/10.1016/j.automatica.2014.02.017

Du, M., Scott, J., & Mhaskar, P. (2013). Actuator and sensor fault isolation of nonlinear process systems. *Chemical Engineering Science*, *104*, 294–303. https://doi.org/10.1016/j.ces.2013.08.009

Edwards, C., Spurgeon, S. K., & Patton, R. J. (2000). Sliding mode observers for fault detection and isolation. *Automatica*, *36*(4), 541–553. https://doi.org/10.1016/S0005-1098(99)00177-6

Ferdowsi, H., Jagannathan, S., & Zawodniok, M. (2014). An online outlier identification and removal scheme for improving fault detection performance. *IEEE Transactions on Neural Networks and Learning Systems*, *25*(5), 908–919. https://doi.org/10.1109/TNNLS.2013.2283456

Ferrari, R. M., Parisini, T., & Polycarpou, M. M. (2009). Distributed fault diagnosis with overlapping decompositions: An adaptive approximation approach. *IEEE Transactions on Automatic Control*, *54*(4), 794–799. https://doi.org/10.1109/TAC.2008.2009591

Huang, Y., Gertler, J., & McAvoy, T. J. (2000). Sensor and actuator fault isolation by structured partial PCA with nonlinear extensions. *Journal of Process Control*, *10*(5), 459–469. https://doi.org/10.1016/S0959-1524(00)00021-4

Ioannou, P. A., & Sun, J. (1996). *Robust adaptive control*. Prentice Hall.

Isermann, R. (2006). *Fault-diagnosis systems: An introduction from fault detection to fault tolerance*. Springer Science & Business Media.

Jia, J., Trentelman, H. L., & Camlibel, M. K. (2020). Fault detection and isolation for linear structured systems. *IEEE Control Systems Letters*, *4*(4), 874–879. https://doi.org/10.1109/LCSYS.7782633

Jung, D., Khorasgani, H., Frisk, E., Krysander, M., & Biswas, G. (2015). Analysis of fault isolation assumptions when comparing model-based design approaches of diagnosis systems. *IFAC-PapersOnLine*, *48*(21), 1289–1296. https://doi.org/10.1016/j.ifacol.2015.09.703

Keliris, C., Polycarpou, M. M., & Parisini, T. (2013). A distributed fault detection filtering approach for a class of interconnected continuous-time nonlinear systems. *IEEE Transactions on Automatic Control*, *58*(8), 2032–2047. https://doi.org/10.1109/TAC.2013.2253231

Keliris, C., Polycarpou, M. M., & Parisini, T. (2015a). Distributed fault diagnosis for process and sensor faults in a class of interconnected

input–output nonlinear discrete-time systems. *International Journal of Control*, *88*(8), 1472–1489. https://doi.org/10.1080/00207179.2015.1007395

Keliris, C., Polycarpou, M. M., & Parisini, T. (2015b). A robust nonlinear observer-based approach for distributed fault detection of input–output interconnected systems. *Automatica*, *53*, 408–415. https://doi.org/10.1016/j.automatica.2015.01.042

Keliris, C., Polycarpou, M. M., & Parisini, T. (2017). An integrated learning and filtering approach for fault diagnosis of a class of nonlinear dynamical systems. *IEEE Transactions on Neural Networks and Learning Systems*, *28*(4), 988–1004. https://doi.org/10.1109/TNNLS.2015.2504418

Khalili, M., Zhang, X., Cao, Y., Polycarpou, M. M., & Parisini, T. (2019). Distributed fault-tolerant control of multiagent systems: An adaptive learning approach. *IEEE Transactions on Neural Networks and Learning Systems*, *31*(2), 420–432. https://doi.org/10.1109/TNNLS.5962385

Kościelny, J. M. (1995). Fault isolation in industrial processes by the dynamic table of states method. *Automatica*, *31*(5), 747–753. https://doi.org/10.1016/0005-1098(94)00147-B

Koscielny, J. M., & Bartys, M. (2009). Application of the method of dynamic decomposition for recognition of multiple faults in the large scale systems. In *7th Workshop on Advanced Control and Diagnostics ACD* (pp. 19–20). http://doi.org/10.13140/2.1.4776.5440.

Koscielny, J. M., Bartys, M., & Ł Syfert, M. (2011). Method of multiple fault isolation in large scale systems. *IEEE Transactions on Control Systems Technology*, *20*(5), 1302–1310. https://doi.org/10.1109/TCST.2011.2162587

Kougiatsos, N., Negenborn, R. R., & Reppa, V. (2022). Distributed model-based sensor fault diagnosis of marine fuel engines. *IFAC-PapersOnLine*, *55*(6), 347–353. https://doi.org/10.1016/j.ifacol.2022.07.153

Li, P., Boem, F., Pin, G., & Parisini, T. (2017). Distributed fault detection and isolation for interconnected systems: A non-asymptotic kernel-based approach. *IFAC-PapersOnLine*, *50*(1), 1013–1018. https://doi.org/10.1016/j.ifacol.2017.08.209

Mao, Z., Wang, Y., Jiang, B., & Tao, G. (2016). Fault diagnosis for a class of active suspension systems with dynamic actuators' faults. *International Journal of Control, Automation and Systems*, *14*(5), 1160–1172. https://doi.org/10.1007/s12555-014-0552-z

Meskin, N., & Khorasani, K. (2009). Actuator fault detection and isolation for a network of unmanned vehicles. *IEEE Transactions on Automatic Control*, *54*(4), 835–840. https://doi.org/10.1109/TAC.2008.2009675

Nemati, F., Hamami, S. M. S., & Zemouche, A. (2019). A nonlinear observer-based approach to fault detection, isolation and estimation for satellite formation flight application. *Automatica*, *107*, 474–482. https://doi.org/10.1016/j.automatica.2019.06.007

Papadopoulos, P. M., Reppa, V., Polycarpou, M. M., & Panayiotou, C. G. (2017). Distributed diagnosis of actuator and sensor faults in HVAC systems. *IFAC-PapersOnLine*, *50*(1), 4209–4215. https://doi.org/10.1016/j.ifacol.2017.08.816

Phatak, M. S., & Viswanadham, N. (1988). Actuator fault detection and isolation in linear systems. *International Journal of Systems Science*, *19*(12), 2593–2603. https://doi.org/10.1080/00207728808547135

Polycarpou, M. M., & Helmicki, A. J. (1995). Automated fault detection and accommodation: A learning systems approach. *IEEE Transactions on Systems, Man, and Cybernetics*, *25*(11), 1447–1458. https://doi.org/10.1109/21.467710

Reppa, V., Polycarpou, M. M., & Panayiotou, C. G. (2014a). Decentralized isolation of multiple sensor faults in large-scale interconnected nonlinear systems. *IEEE Transactions on Automatic Control*, *60*(6), 1582–1596. https://doi.org/10.1109/TAC.2014.2384371

Reppa, V., Polycarpou, M. M., & Panayiotou, C. G. (2014b). Distributed sensor fault diagnosis for a network of interconnected cyberphysical systems. *IEEE Transactions on Control of Network Systems*, *2*(1), 11–23. https://doi.org/10.1109/TCNS.2014.2367362

Reppa, V., Polycarpou, M. M., & Panayiotou, C. G. (2016). Sensor fault diagnosis. *Foundations and Trends in Systems and Control*, *3*(1–2), 1–248.

Riverso, S., Boem, F., Ferrari-Trecate, G., & Parisini, T. (2016). Plug-and-play fault detection and control-reconfiguration for a class of nonlinear large-scale constrained systems. *IEEE Transactions on Automatic Control*, *61*(12), 3963–3978. https://doi.org/10.1109/TAC.2016.2535724

Rymon, R. (1993). An SE-tree based characterization of the induction problem. In *International Conference on Machine Learning* (pp. 268–275). Morgan Kaufmann.

Talebi, H. A., Khorasani, K., & Tafazoli, S. (2009). A recurrent neural-network-based sensor and actuator fault detection and isolation for nonlinear systems with application to the satellite's attitude control subsystem. *IEEE Transactions on Neural Networks*, *20*(1), 45–60. https://doi.org/10.1109/TNN.2008.2004373

Thumati, B. T., & Jagannathan, S. (2010). A model-based fault-detection and prediction scheme for nonlinear multivariable discrete-time systems with asymptotic stability guarantees. *IEEE Transactions on Neural Networks*, *21*(3), 404–423. https://doi.org/10.1109/TNN.2009.2037498

Trunov, A. B., & Polycarpou, M. M. (2000). Automated fault diagnosis in nonlinear multivariable systems using a learning methodology. *IEEE Transactions on Neural Networks*, *11*(1), 91–101. https://doi.org/10.1109/72.822513

Wang, H., Huang, Z. J., & Daley, S. (1997). On the use of adaptive updating rules for actuator and sensor fault diagnosis. *Automatica*, *33*(2), 217–225. https://doi.org/10.1016/S0005-1098(96)00155-0

Wu, Q., & Saif, M. (2007). Robust fault detection and diagnosis in a class of nonlinear systems using a neural sliding mode observer. *International Journal of Systems Science*, *38*(11), 881–899. https://doi.org/10.1080/00207720701628889

Xu, F., Tan, J., Wang, X., Puig, V., Liang, B., & Yuan, B. (2017). Mixed active/passive robust fault detection and isolation using set-theoretic unknown input observers. *IEEE Transactions on Automation Science and Engineering*, *15*(2), 863–871. https://doi.org/10.1109/TASE.2017.2776998

Yan, X. G., & Edwards, C. (2008a). Robust sliding mode observer-based actuator fault detection and isolation for a class of nonlinear systems. *International Journal of Systems Science*, *39*(4), 349–359. https://doi.org/10.1080/00207720701778395

Yan, X. G., & Edwards, C. (2008b). Robust decentralized actuator fault detection and estimation for large-scale systems using a sliding mode observer. *International Journal of Control*, *81*(4), 591–606. https://doi.org/10.1080/00207170701536056

Yin, X., & Liu, J. (2017, May). Distributed fault detection and isolation of nonlinear systems using output feedback. In *2017 6th International Symposium on Advanced Control of Industrial Processes (AdCONIP)* (pp. 547–552). IEEE.

Zhang, L., Hua, C., Cheng, G., Li, K., & Guan, X. (2020). Decentralized adaptive output feedback fault detection and control for uncertain nonlinear interconnected systems. *IEEE Transactions on Cybernetics*, *50*(3), 935–945. https://doi.org/10.1109/TCYB.6221036

Zhang, P., Ding, S. X., & Liu, P. (2012). A lifting based approach to observer based fault detection of linear periodic systems. *IEEE Transactions on Automatic Control*, *57*(2), 457–462. https://doi.org/10.1109/TAC.2011.2166712

Zhang, X. (2011). Sensor bias fault detection and isolation in a class of nonlinear uncertain systems using adaptive estimation. *IEEE Transactions on Automatic Control*, *56*(5), 1220–1226. https://doi.org/10.1109/TAC.2011.2112471

Zhang, X., Polycarpou, M. M., & Parisini, T. (2002). A robust detection and isolation scheme for abrupt and incipient faults in nonlinear systems. *IEEE Transactions on Automatic Control*, *47*(4), 576–593. https://doi.org/10.1109/9.995036

Zhang, X., & Zhang, Q. (2012). Distributed fault diagnosis in a class of interconnected nonlinear uncertain systems. *International Journal of Control*, *85*(11), 1644–1662. https://doi.org/10.1080/00207179.2012.696146

Zhang, Z., & He, X. (2022). Robust fault diagnosis for uncertain linear systems: A set-based geometric approach. *IEEE Transactions on Instrumentation and Measurement*, *71*, 1–9.

Zhao, X., & Ouyang, D. (2007, August). Improved algorithms for deriving all minimal conflict sets in model-based diagnosis. In *International Conference on Intelligent Computing* (pp. 157–166). Springer.